https://doi.org/10.1016/j.ejmech.2018.12.029

Translational impact of novel widely pharmacological characterized mofezolac-derived COX-1 inhibitors combined with bortezomib on human multiple myeloma cell lines viability

Maria Laura Pati[a,1], Paola Vitale[a,1], Savina Ferorelli[a], Mariaclara Iaselli[a], Morena Miciaccia[a], Angelina Boccarelli[b], Giuseppe Davide Di Mauro[c], Cosimo G. Fortuna[c], Thaisa Francielle Souza Domingos[d], Luiz Claudio Rodrigues Pereira da Silva[d], Marcelo de Padula[d], Lucio Mendes Cabral[d], Plínio Cunha Sathler[d], Angelo Vacca[e], Antonio Scilimati[a,**], Maria Grazia Perrone[a,*]

[a] Department of Pharmacy - Pharmaceutical Sciences, University of Bari "Aldo Moro", Via E. Orabona 4, 70125, Bari, Italy
[b] Department of Biomedical Sciences and Human Oncology, University of Bari "Aldo Moro", Piazza Giulio Cesare 11, 70124, Bari, Italy [c] Department of Chemical Science, University of Catania, Viale Andrea Doria 6, 95125, Catania, Italy
[d] Faculty of Pharmacy, Federal University of Rio de Janeiro, Center of Health Sciences, Carlos Chagas Filho Avenue, 373, 21941599, Rio de Janeiro, Brazil
[e] Department of Biomedical Sciences and Human Oncology, Internal Medicine Unit G. Baccelli, University of Bari Aldo Moro Medical School, Bari, Italy

Keywords:
Cyclooxygenase
Selective COX-1 inhibition
Mofezolac
Structure-inhibitory activity relationships in silico investigation
Bortezomib
Multiple myeloma

abstract

A set of novel diarylisoxazoles has been projected using mofezolac (1) as a lead compound to investigate structure-inhibitory activity relationships of new compounds and the cyclooxygenases (COXs) catalytic activity. Mofezolac was chosen because is the most potent and selective reversible COX-1 inhibitor [COX-1 IC_{50} ¼ 0.0079 mM and COX-2 IC_{50} > 50 mM, with a selectivity index (SI) in favor of COX-1 higher than 6300]. Seventeen new compounds were synthesized in fair to good yields and evaluated for their COXs inhibitory activity and selectivity. SIs ranged between 1 and higher than 1190.3,4-Bis(4-methoxyphenyl)-5-vinylisoxazole (22) has the highest SI with COX-1 IC_{50} ¼ 0.042 mM and COX-2 IC_{50} > 50 mM. 1 and 22 were superior to aspirin in inhibiting platelet aggregation (IC_{50} ¼ 0.45, 0.63 and 1.11 mM, respectively) in human platelet rich plasma (hPRP) assay. They did not induce blood coagulation and hemolysis, and are neither genotoxic nor mutagen. 1 and 22 slightly increase bortezomib cytotoxic effect on multiple myeloma (MM) cell lines (NCI-H929 and RPMI-8226) and affects MM cell cycle and apoptosis when co-administered with the proteasome inhibitor bortezomib, a drug clinically used to treat plasma cell neoplasms including MM. In addition, structure-based binding mode of 1 and 22, through Fingerprints for Ligands and Proteins (FLAG) calculation, allowed to explain the one order of magnitude difference between COX-1 IC_{50} values of the two compounds. Specifically, the higher inhibitory potency seems due to the formation of a H-bond between COX-1 S530 and the carboxyl, present in 1 and absent in 22.

1. Introduction

Non-Steroidal Anti-inflammatory Drugs (NSAIDs) are the most used drugs to treat inflammatory syndrome, fever, pain, and rheumatic pathologies. NSAIDs therapeutic and side effects are mainly due to the inhibition of prostaglandins biosynthesis, that starts with the bis-oxygenation of arachidonic acid (AA) catalyzed by the cyclooxygenase (COX) isoenzymes, in which the first formed prostaglandin PGG_2 is converted into the PGH_2, in turn precursor of the PGI_2, PGE_2, thromboxane $(TX)A_2$ and other eicosanoids [1]. Prostaglandins are crucial mediators of inflammation [2], regulators of platelet function and hemostasis [3], angiogenesis [4] and support the growth of several solid tumors [5].

* Corresponding author.
** Corresponding author.
E-mail addresses: antonio.scilimati@uniba.it (A. Scilimati), mariagrazia.perrone@uniba.it (M.G. Perrone).
[1] M. L. Pati and P. Vitale have equally contributed to this project.

Two COXs isoforms are known, COX-1 and COX-2. Their expression is either constitutive or inducible, depending on the organ considered and specific physio-pathological established condition [6]. In particular, COX-2 expression is constitutive in liver and brain, and in almost all body districts where it is induced in response to inflammatory stimuli and growth factors upon various pathological conditions in which the inflammation is the committed earliest stage [7], including cancer and, neurological and neurodegenerative diseases [8e12]. COX-1 plays homeostatic function in most tissues (e.g. platelets, lung, prostate, brain, gastrointestinal tract, kidney, liver and spleen), where it is constitutively expressed, and its overexpression is rarely observed [1]. Experimental evidences proven COX-1 expressed and involved in different tumors such as breast [13], ovarian [14], head and neck [15] cancer, renal cell carcinoma [16], and hematological (i.e., multiple myeloma) tumors [17] for which it could be considered as a biomarker of a diagnostic value.

Multiple myeloma (MM) is a tumor that affects the plasma cells, key components of the immune system. MM is also characterized as a clonal proliferation of neoplastic plasma cells in the bone marrow (BM) and accounts for 30% of all hematological malignancies [18]. Nowadays, bortezomib, a proteasome inhibitor, or immunomodulators such as lenalidomide and thalidomide are used to treat MM. The effect of bortezomib, the first proteasome inhibitor to be approved by the Food and Drug Administration in 2003, is well recognized. At present, bortezomib is the first- and second-line treatment in MM. However, the increasing administration of bortezomib is associated with the development of drug resistance [19].

Due to the high risk of thromboembolism, as a heavy side effect, associated to the above mentioned immunomodulators [20,21] or proteasome inhibitor treatment, MM patients preventively hire also aspirin (Fig. 1) [22].

Nearly all MM patients experience relapse and refractory disease [23]. Aspirin use, along with reducing the incidence of thrombotic complications also improves overall survival, by producing additive or synergistic effects in the treatment of MM because enhances bortezomib cytotoxicity via suppression of Bcl-2, survivin and AKT phosphorylation [24].

Low dose-aspirin anti-thrombotic effect is mainly due to the irreversible inhibition of platelet COX-1 catalytic activity by acetylation of COX-1 Ser530, that permanently blocks the AA binding inside the enzyme active site.

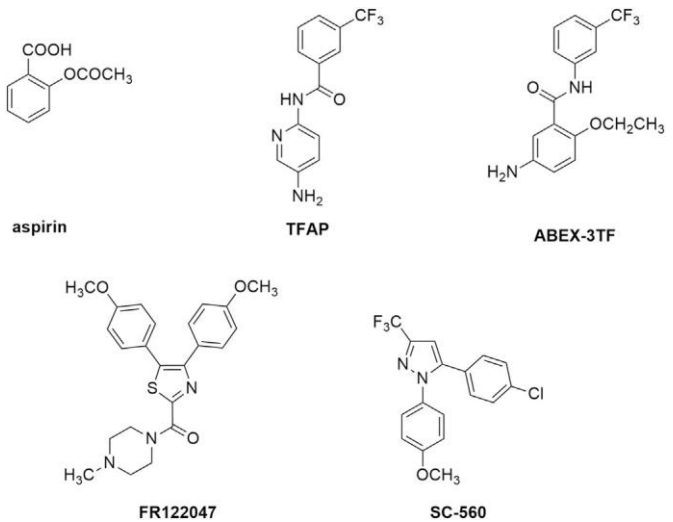

Fig. 1. Aspirin and COX-1 selective inhibitors.

Platelets are almost unable to replace inactive acetyl-COX-1 being anucleated. Thus, daily aspirin hiring has a therapeutic advantage against thrombosis acting by inhibiting any COX-1 mediated reaction. Unfortunately, variability in the sensitivity of patients to aspirin interferes with the necessary complete and persistent suppression of TXA_2 biosynthesis in cardio-protection, by causing among other factors COX-1 dependent "aspirin resistance" [25].

The use of aspirin is also restricted, since it causes either patient-hypersensitivity or -intolerance in up to 20% of the worldwide population [26].

Aspirin resistance, hypersensitivity and intolerance limit the aspirin use. Therefore, COX-1 inhibitors alternative to aspirin are needed.

An increasing number of selective COX-1 inhibitors has been found, such as TFAP, ABEX-3TF, FR122047, SC-560, P6 and mofezolac (Figs. 1 and 2)]. Among them, mofezolac is the unique marketed drug, sold in Japan as Disopain® to relieve rheumatoid arthritis pain [1].

Most of the highly selective COX-1 inhibitors belong to the diarylheterocycle chemical class, and among them the isoxazole has specifically been used as central ring in the structure of mofezolac, P6 [3-(5-chlorofuran-2-yl)-5-methyl-4-phenylisoxazole] and its analogues, and valdecoxib (conversely, is a selective COX-2 inhibitor) (Fig. 2) [27].

P6 and mofezolac belong to isoxazole-scaffold based COX-1 inhibitors: P6 bears a methyl on C5, a phenyl on the isoxazole-C4 and a 5-chlorofuranyl on isoxazole-C3, whereas two 4-methoxyphenyls are linked to mofezolac central heterocyclic ring, that possesses an acidic moiety on C5. Valdecoxib chemical structure has a phenyl on the isoxazole-C3, a methyl on isoxazole-C5, and differs mainly from P6 and mofezolac for the presence of a sulfonamide group on the para position of the isoxazole-C4 phenyl, that seems responsible of the reversal of the selectivity in favor of COX-2 (Fig. 2). The presence of an acidic moiety (-CH_2COOH) at mofezolac C5 seems to be important for the high inhibitory potency and COX-1 selectivity, mainly due to its strong interaction with R120 located at entrance of the COX-1 catalytic site [28].

A number of diarylheterocycles with a different central ring has been previously prepared with the aim to clarify the importance of the isoxazole for the selective COX-1 inhibition by P6 and its analogues. In particular, the isoxazole replacement by isothiazole or pyrazole determines a remarkable inhibitory activity reduction of the corresponding diarylisothiazoles and diarylpyrazoles in the COX-1 catalyzed AA bis-oxygenation reaction [29].

In this regard, differently substituted 3,4-diarylisoxazoles were prepared and tested as COX-1 and COX-2 isoenzymes inhibitors for an extensive structure-inhibitory activity relationship investigation [30,31]. Based on the obtained results some compound key features appeared determinant to selectively inhibit COX-1 (Fig. 3).

Specifically, in the presence of a methyl, bromo or chloro-substituted furan linked to the isoxazole-C3, the aromatic moiety at the isoxazole-C4 can be a phenyl or an aryl bearing electron-donating group (EDG) capable of þM effect (o- or p-halophenyl, p-aminophenyl, or p-methoxyphenyl); a variety of substituents are well-tolerated at isoxazole-C5 position such as short alkyl chains, CF_3, hydroxymethyl, amino groups (Fig. 3) [27,32].

As an attempt to still validate these findings, herein, we describe a new set of isoxazoles designed taking into account the already identified determinants. The novel compounds were projected also with further additional functionalities as an attempt to target diseases such as multiple myeloma [20,21,33], thrombosis [34], and ovarian cancer [14].

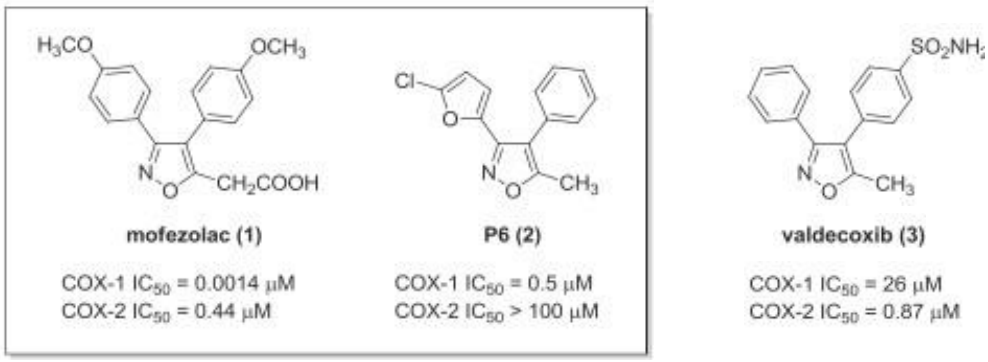

Fig. 2. Isoxazole-scaffold based COXs inhibitors. Mofezolac IC_{50} values are determined by seminal vesicles, whereas P6 and valdecoxib IC_{50} values are by human whole blood assay [1].

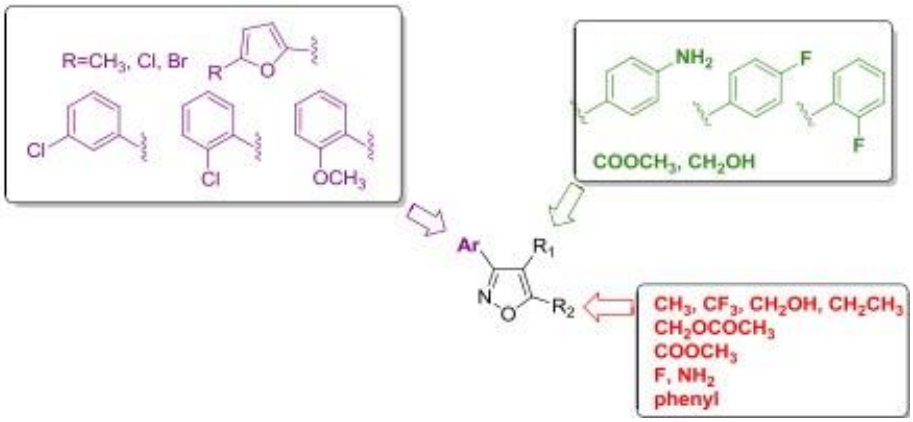

Fig. 3. Key chemical moieties determinant isoxazole-based scaffold for selective COX-1 inhibitors.

2. Results and discussion

A first set of molecules was designed as diarylisoxazolyl-5-acetic acids, in analogy to mofezolac (1, oCOX-1 IC_{50} ¼ 0.0079 mM and hCOX-2 IC_{50} > 50 mM), whereas the second set derived from the 5-amino-3-(5-chlorofuran-2-yl)-4-phenylisoxazole (27) used as a "lead compound" [oCOX-1 IC_{50} ¼ 1.1 mM and hCOX-2 IC_{50} > 50 mM, and with COX-1 IC_{50} ¼ 0.58 mM inhibitory activity assessed in the human ovarian cancer cell line hOVCAR-3 expressing only the COX-1 isoform [35]. The main difference between mofezolac and 27 is the presence at isoxazole-C5 of an acid (acetic group) in mofezolac and a basic (amino group) in 27.

The isoxazoles 8e12 have been prepared by a "one-pot" 1,3-dipolar cycloaddition of substituted arylnitrile oxides 6a-c and 6e (Scheme 1) and the sodium enolate of arylpropanones 7 generated at 0 C by deprotonation of the corresponding ketones with NaH under thermodynamic conditions (Scheme 2) [34e36]. Specifically, arylnitrile oxides were prepared by dehydrohalogenation of benzohydroximinoyl chlorides 5a-c and 5e in turn obtained from the corresponding oximes 4a-c and 4e (Scheme 1).

Reduction of the nitro group of the isoxazole 12 by stannous chloride in hydrochloric acid provides 13 [35], that by reacting with acetic anhydride affords 14 (Scheme 3).

3,4-Diaryl-5-methylisoxazoles 8,10, 13e14 were treated with n-BuLi under nitrogen atmosphere and kept at 78 C for 1h. Then, anhydrous CO_2 was bubbled into the lithiated intermediates still at 78 C, to afford the corresponding diarylisoxazolyl acetic acids 1 (mofezolac) [28] and 15e17 (Scheme 4) after quenching with HCl.

3,4-Bis(4-methoxyphenyl)-5-(bromomethyl)isoxazole (18) was prepared by bromination of 8 with N-bromosuccinimide (NBS) in the presence of azobisisobutyronitrile (AIBN) as a radical initiator. Then, 18 reacted with anhydrous tetrabutylammonium fluoride (TBAF) to afford 19 (Scheme 5).

The alcohol 20 was obtained by reducing the carboxylic moiety of mofezolac in the presence of borane. 20 was transformed into its tosylate 21 by reaction with Ts_2O in the presence of Et_3N, and then

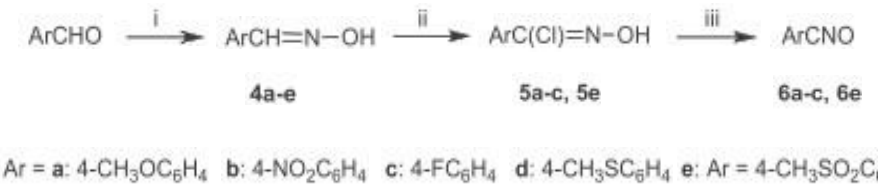

Scheme 1. Synthesis of the arylnitrile oxides 6a-c, 6e. Reagent and conditions: (i) NH_2OH HCl/aq. NaOH, EtOH, quantitative yield; (ii) N-chlorosuccinimide, DMF; (iii) Et_3N/THF, quantitative yield.

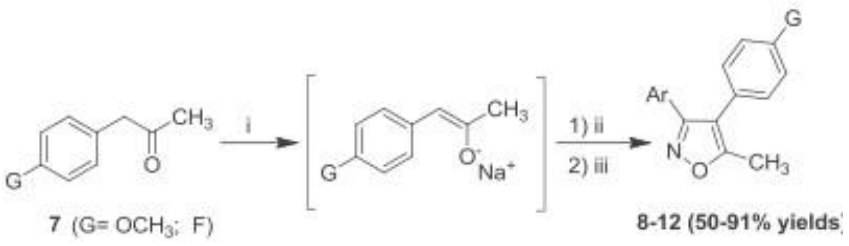

8: Ar = 4-$CH_3OC_6H_4$, G= OCH_3; **9**: Ar = 4-$NO_2C_6H_4$, G = F; **10**: Ar = 4-FC_6H_4, G = OCH_3;
11: Ar = 4-$CH_3SO_2C_6H_4$, G = F; **12**: Ar = 4-$NO_2C_6H_4$, G = OCH_3.

Scheme 2. Synthesis of diarylisoxazoles 8e12. Reagent and conditions: (i) NaH/THF, 0 C; (ii) arylnitrile oxide (ArCNO)/THF, from 0 C to r.t.; (iii) aq. NH_4Cl.

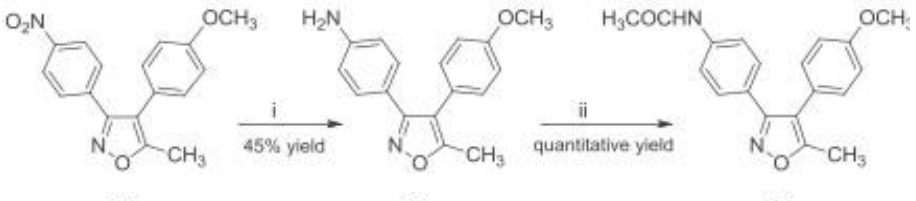

Scheme 3. Synthesis of 13e14. Reagents and conditions: (i) $SnCl_2$/HCl, EtOH, 24h; (ii) Ac_2O/Py, r.t.

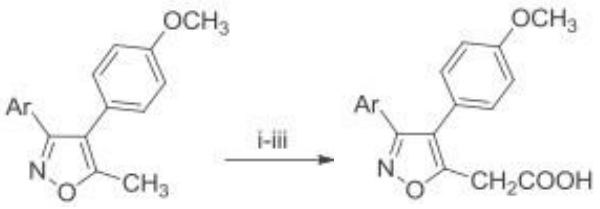

Ar = **8** and **1**: 4-$OCH_3C_6H_4$; **10** and **15**: 4-F-C_6H_4
13 and **16:** 4-$NH_2C_6H_4$; **14** and **17:** 4-$CH_3CONHC_6H_4$

Scheme 4. Synthesis of diarylisoxazolyl acetic acids 1, 15e17. Reagents and conditions: (i) n-BuLi, 78 C, 1h; (ii) CO_2 (g), from 78 C to r.t.; (iii) 0.1M HCl.

the 5-vinylisoxazole 22 formed by beta-elimination induced by TBAF (Scheme 6).

5-Amino-3,4-diarylisoxazoles 23e26 were prepared by a one-pot methodology, through a cycloaddition reaction between aryl-nitrile oxides and lithium arylacetonitriles [37] (Scheme 7):

All the novel isoxazoles were evaluated in vitro against oCOX-1 and hCOX-2 to determine their COXs IC_{50} values (Table 1).

Mofezolac (1), one of our "leads" used as reference compound for this SAR investigation has a selective COX-1 inhibitory activity (IC_{50} ¼ 0.0079 mM) at nanomolar level. The absence of the acidic function on isoxazole-C5, as in compound 8, leads to a preferential but non-selective COX-1 inhibitor, and also less potent (COX-1 IC_{50} ¼ 0.076 mM and COX-2 IC_{50} ¼ 0.35 mM, selectivity index SI ¼ 4.6). The introduction of a nitro group on the phenyl linked to the isoxazole-C3 was found to be detrimental to 9 and 12 inhibitory activity of both cyclooxygenase isoforms. Particularly interesting is the introduction of a vinyl group to the isoxazole-C5, in compound 22, found to be selective and potent COX-1 inhibitor (SI > 1190). The substitution of the carboxyl with a hydroxyl determines a reduction of the COXs inhibitory activity of 20 (COX-1 IC_{50} ¼ 0.12 mM, COX-2 IC_{50} ¼ 0.19 mM, SI ¼ 1.6) compared to 1. Metabolically, 20 could be considered the precursor of mofezolac (1). The coexistence of two methoxyphenyls and a -CH_2X [X ¼ bromine (18) or fluorine (19)] on isoxazole-C5 led to a submicromolar COX-1 inhibitor potency (0.10 and 0.35 mM, respectively) but also to a lost in selectivity. In fact, both halo-compounds inhibit COX-2 with an IC_{50} of 0.18 and 0.3 mM for compound 18 and 19, respectively. The presence of a fluorine as a substituent of the aryl group in position C3 of the isoxazole leads to selective COX-1 inhibitors (10, 15, and 24) with a partial loss of inhibitory potency. In fact, compound 15, which is different from the lead compound (1) only for the substitution of a methoxy group with a fluorine atom remains a selective COX-1 inhibitor, but its IC_{50} ¼ 7.5 mM is lower of three orders of magnitude than 1. When the acidic function is also replaced with a basic amino group (24), the inhibitory potency is further reduced (IC_{50} ¼ 13 mM), probably due to the simultaneous presence of a fluorine atom and NH_2 group leads to micromolar COX-1 inhibitors potency. COX-1 inhibitory

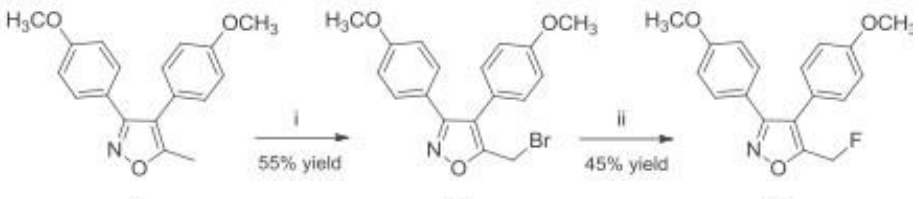

Scheme 5. Preparation of 5-halomethylisoxazoles 18e19. Reagents and conditions: (i) N-bromosuccinimide/azobisisobutyronitrile/CCl_4; (ii) anhydrous tetrabutylammonium fluoride/THF.

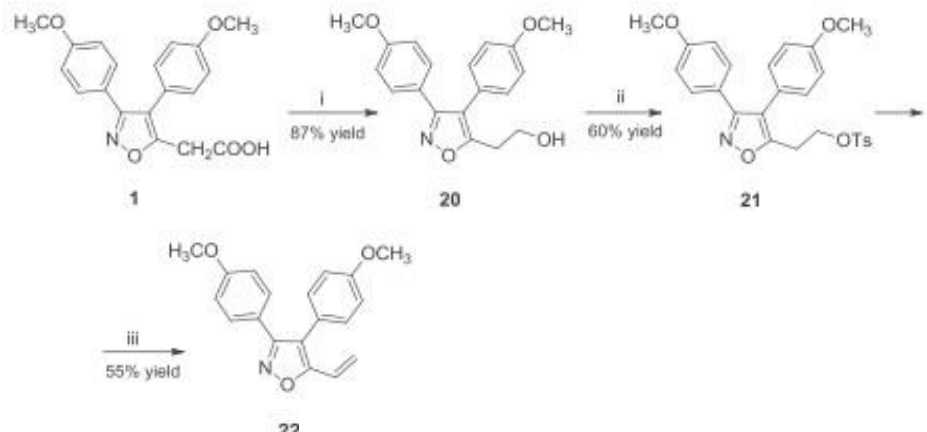

Scheme 6. Synthesis of the target 20 and 22. Reagents and conditions: (i) BMS/THF at 0 C to r.t.; (ii) Ts_2O, Et_3N at 0 C to r.t.; (iii) TBAF/THF, r.t.

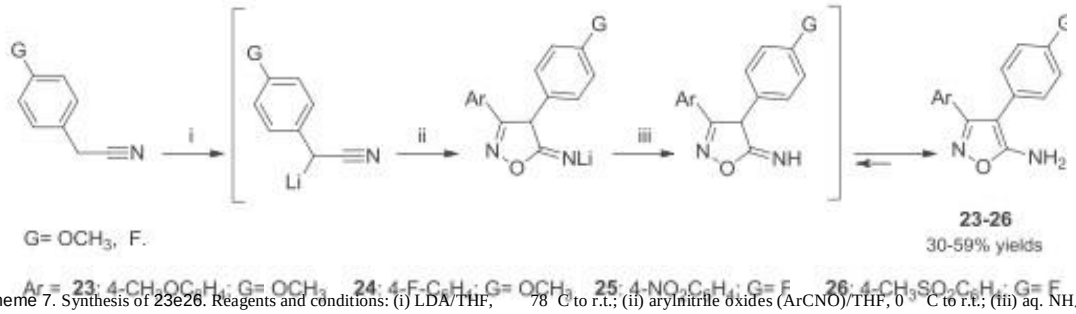

Scheme 7. Synthesis of 23e26. Reagents and conditions: (i) LDA/THF, 78 C to r.t.; (ii) arylnitrile oxides (ArCNO)/THF, 0 C to r.t.; (iii) aq. NH_4Cl.

Table 1
COX inhibitory activity of isoxazoles 8e13, 15e20, 22e28 and mofezolac (1) used as a reference compound.

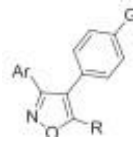

Compound	Ar	G	R	COX-1 IC_{50} (mM)[a]	COX-2 IC_{50} (mM)[a]
1	4-$CH_3OC_6H_4$	OCH_3	CH_2COOH	0.0079	>50
8	4-$CH_3OC_6H_4$	OCH_3	CH_3	0.076	0.35
9	4-$NO_2C_6H_4$	F	CH_3	>50	>50
10	4-FC_6H_4	OCH_3	CH_3	3 (94)	>50
11	4-$CH_3SO_2C_6H_4$	F	CH_3	>50 (24)	0.07 (52)
12	4-$NO_2C_6H_4$	OCH_3	CH_3	36% at 10 mM	>50
13	4-$NH_2C_6H_4$	OCH_3	CH_3	23 (53)	>50
15	4-FC_6H_4	OCH_3	CH_2COOH	7.5 (92)	>50
16	4-$NH_2C_6H_4$	OCH_3	CH_2COOH	>50 (33)	>50 (42)
17	4-$CH_3CONHC_6H_4$	OCH_3	CH_2COOH	12 (79)	>50
18	4-$CH_3OC_6H_4$	OCH_3	CH_2Br	0.10 (93)	0.18 (63)
19	4-$CH_3OC_6H_4$	OCH_3	CH_2F	0.35 (100)	0.3 (85)
20	4-$CH_3OC_6H_4$	OCH_3	CH_2CH_2OH	0.12 (100)	0.19 (82)
22	4-$CH_3OC_6H_4$	OCH_3	CH¼CH_2	0.042 (100)[b]	>50[b]
23	4-$CH_3OC_6H_4$	OCH_3	NH_2	8.3 (89)	>50
24	4-FC_6H_4	OCH_3	NH_2	13 (83)	>50
25	4-$NO_2C_6H_4$	F	NH_2	12 (71)	>50
26	4-$CH_3SO_2C_6H_4$	F	NH_2	>50	>50
27[c]	5-chlorofuran-2-yl	H	NH_2	1.1	>50
28[c]	5-chlorofuran-2-yl	NH_2	CH_3	4.3	>50

[a] In round brackets is reported the inhibition percentage (%) of the isoenzyme activity at the compound final concentration of 50 mM; b) Selective Index, SI ¼ COX-2 IC_{50}/ COX-1 IC_{50} > 1190; c) [35].

activity (IC_{50} ¼ 3.0 mM) of 10 is comparable to that of its acid derivative 15, indicating that the presence of a fluorine contributes to COX-1 selectivity but not to the potency of the novel synthesized diarylisoxazoles.

On the other hand, the presence of NH_2 group is determinant in the interaction with COX-1 active site because it forms strong H-bond with COX-1 Ser 530, which adopts a "down" position during the flexible docking simulation and it does not matter if the NH_2 is

bound to the isoxazole-C5 (23, 25 and 27) or to the phenyl at isoxazole-C4 (28) [35]. Comparing 25 and 9 behavior, there is a further confirmation of our previous studies. Specifically, the absence of the amino group at isoxazole-C5, in compound 9, determines a total loss of COXs inhibitory activity with respect to the compound 25. On the contrary, the introduction of the amino group on the phenyl to isoxazole-C3 is associated with a loss of inhibitory activity (13 and 16). In particular, 16 has been designed to better understand if the position of the amino group has a role in the interaction with the active site of COX-1 and in fact by simply replacing the methoxy group of 1 with an amino group, a COX-1 inhibitor with a nanomolar activity becomes an inactive compound.

By transforming the amino group in an amide, reverting the aminic to acidic characteristic of the moiety (NH_2 to $NHCOCH_3$, compound 17) COX-1 inhibitory activity was restored (IC_{50} ¼ 12 mM). On the other hand, the introduction of a 4-methylsulfamoyl substituent on the phenyl linked to isoxazole-C3 reverts the selectivity, even if it is not a rule [26]. In fact, compound 11 has a COX-2 IC_{50} ¼ 0.07 mM. As it is evident from the data listed in Table 1, among all the synthesized inhibitors, the most potent and selective identified inhibitor is compound 22. To rationalize this outcome, an in silico study using Fingerprints for Ligands and Proteins (FLAP) [38] by using COX-1 co-crystallized with mofezolac (PDB code: 5HQK) has been performed, also to identify fruitful and eventually not yet identified interactions established between 22 and COX-1 aminoacids forming the active site.

Structure-based binding mode. The X-ray structure of the complex COX-1:mofezolac (1) was used as a validated model [28]. First, 1 was removed from the COX-1 template and without any constrain FLAP (Fingerprints for Ligands and Proteins) [38] calculated by GRID molecular interaction fields (a computational procedure for determining energetically favorable binding sites on biological macromolecoles) of 22 in the cavity of COX-1.22 was chosen because it was found to be the best COXs inhibitors of the set above reported (COXs SI > 1190 in favor of COX-1, Table 1). The results of the best arrangement of 22 were analyzed (Fig. 4).

Hydrophobic interactions have been observed between the isoxazole ring and A527, the vinyl group and F518, the phenyl linked to the isoxazole-C3 with L359 and Y355; the phenyl on the isoxazole-C4 with Y355, I523 and L352.

The strongest interaction (violet spot in Fig. 4) is observed between the methoxy of the phenyl on the isoxazole-C4, as a H-bond acceptor, and Y355.

In Fig. 5, the superimposition of mofezolac (1) and 22 in the COX-1 active site is reported.

From the comparison of the best arrangement of both compounds in the active site, analyzing their interactions with specific residues, it is possible to explain the difference between their COX-1 inhibitory activity values: mofezolac (1) (IC_{50} ¼ 0.0079 mM) and 22 (IC_{50} ¼ 0.042 mM). They show a similar orientation in the active site, demonstrated by their common interactions with I523, L352 and Y355, whereas for mofezolac a strong H-bond donor interaction between S530 and the acid group is observed. Probably, such a H-bonding is one of the main factors responsible of mofezolac higher inhibitory activity than 22.

In addition, a further docking investigation was performed to explain the inactivity of 9. Fig. 6 shows as 9 interacts with the active site of the COX-1.

Hydrophobic interactions are observed between the isoxazole ring and L352, the methyl and L531, the phenyl at isoxazole-C3 with F518, L352 and Y355 and, the phenyl on the isoxazole-C4 with Y355 and L531.

The strongest interaction (violet spot in Fig. 6) is observed between the methyl linked to the isoxazole ring and L531.

The best arrangement of both compounds in the active site, allows to explain the difference between their COX-1 inhibitory activity values (Table 1). They have similar orientation in the active site by interacting with L352 and Y355. Mofezolac has a strong H-bond donor interaction between S530 and the acid group, absent in 9. Moreover, mofezolac interacts with I523 and this interaction has not been observed for 9. Probably, such a H-bonding and the interaction with I523 are the main factors responsible for mofezolac higher inhibitory activity than 9 (Fig. 7).

The methoxy substituent is a “key group” in the interaction with COX-1 active site. In our previous investigations, the para-methoxyphenyl of a diarylpyrazole was found oriented toward the apex of the COX-1 active site and formed hydrophobic interactions with residues F518, M522, and I523, whereas its methoxy substituent lies within van der Waals contact range of the side chains of F381, L384, Y385, and W387. Notably, the oxygen atom of the para-methoxy substituent forms two contact points to the W387 side chain. W387 is located at the top of the COX-1 active site near the catalytic Y385 residue that is critical for the proper positioning of

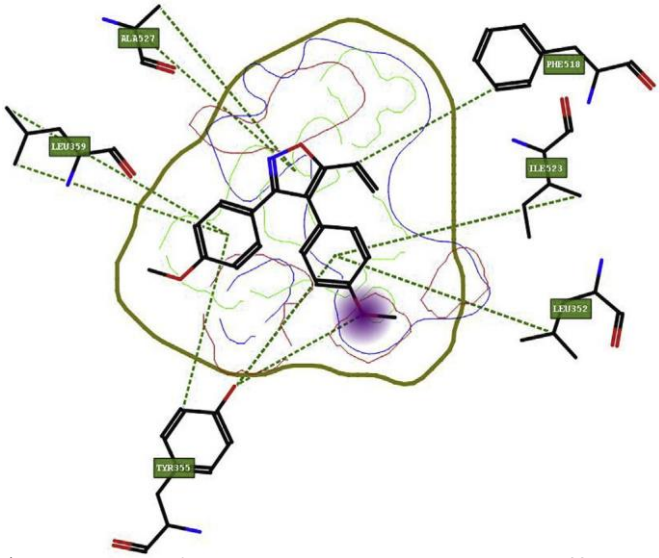

Fig. 4. Arrangement of the 3,4-bis(4-methoxyphenyl)-5-vinylisoxazole (22) in COX-1 active site.

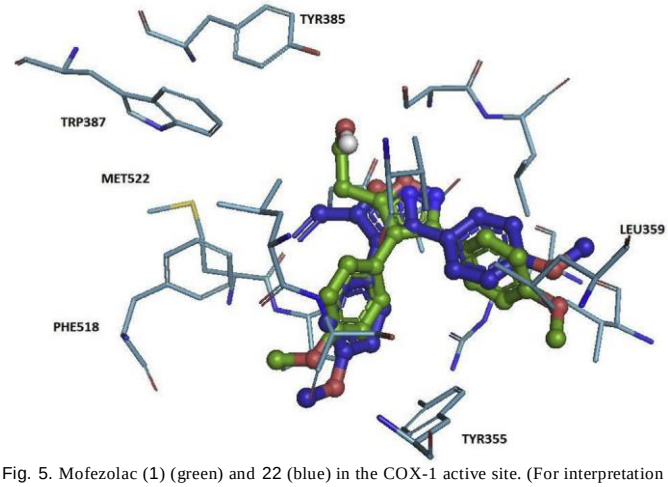

Fig. 5. Mofezolac (1) (green) and 22 (blue) in the COX-1 active site. (For interpretation of the references to color in this figure legend, the reader is referred to the Web version of this article.)

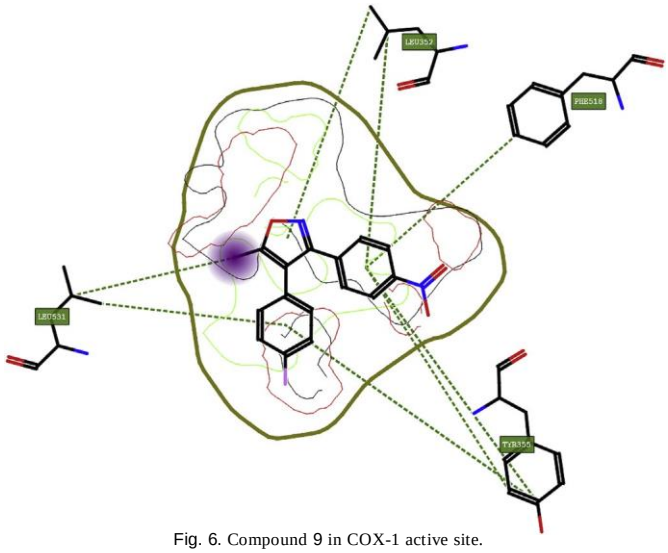

Fig. 6. Compound 9 in COX-1 active site.

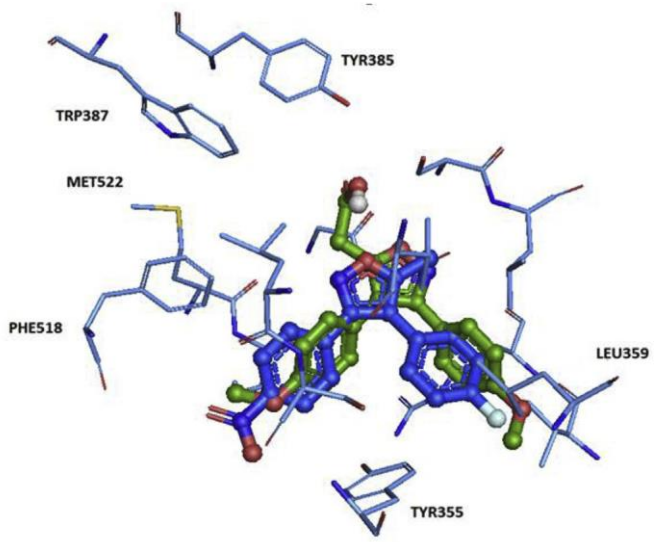

Fig. 7. Mofezolac (1) (green) and 9 (blue) in the active site of COX-1. (For interpretation of the references to color in this figure legend, the reader is referred to the Web version of this article.)

arachidonic acid within the active site to yield the cyclooxygenase-mediated PGG_2.

Pharmacological and toxicological characterization of compounds 1 and 22. Mofezolac (1) and 22 were further characterized by evaluating their contribution in platelet aggregation and blood coagulation, and their hemolytic and genotoxicity effects. In addition, their multiple myeloma cell lines cytotoxicity, apoptosis and cell cycle modification effects has been investigated to verify if these two highly selective COX-1 inhibitors have the same aspirin additive or synergistic effects in the treatment of MM when co-administered with bortezomib, one of the drugs clinically used to treat plasma cell neoplasms including MM [24].

Platelet aggregation assay. The antiplatelet profile of 1, 22 and aspirin (reference compound) have been determined by using an in vitro platelet aggregation method in which platelet aggregation was induced by arachidonic acid (AA) in human citrated platelet rich plasma. 1 and 22 have a comparable potency in inhibiting platelet aggregation. Their IC_{50} are 0.45 ± 0.04 mM and 0.63 ± 0.17 mM, respectively, and better than aspirin (IC_{50} ¼ 1.11 ± 1.17 mM). Thus, 1 and 22, as aspirin, reduce the TXA_2 production by COX-1 inhibition as a part of the mechanism that impair normal platelet aggregation [39].

Anticoagulant assays. Blood anticoagulant profile of 1 and 22 has been determined by activated partial thromboplastin time (APTT) and prothrombin time (PT) using human plasma (Table 2).

Neither the extrinsic nor intrinsic pathways of the coagulation cascade were affected by 1 and 22, suggesting that their anti-hemostatic profile relies on the direct impairment of platelet aggregation, thus differing from dual action molecules (Table 2). This result reveals a small bleeding risk in comparison to dual acting molecules whose mechanism often leads to severe bleeding disorders [40,41].

Hemolytic activity. The hemolytic activity of 1 and 22 in comparison to aspirin was investigated and results are listed in Table 3.

The hemocompability profile for the compounds was determined based on the degree of erythrocyte lysis observed in the 3h incubation period at 37 C. Hemolysis values below 10% are considered non-hemolytic, confirming an acceptable toxicity profile of the tested compounds [42].

Mutagenic and genotoxic activity. The safety profile of 1 and 22 is reinforced by genotoxicity tests which revealed no mutagenicity against Salmonella typhimurium auxotroph mutant strains for the two compounds through reverse mutagenesis and histidine prototrophy (Ames test), compared to the positive control 4-nitroquinoline 1-oxide (4-NQO), nor genotoxicity, evaluated against Escherichia coli through the SOS chromotest. This low risk profile is maintained even at the highest tested concentration (500 mM, Table 4), revealing the safety profile of 1 and 22 as promising for "lead prototypes".

Western blotting. Based on our best knowledge, the expression of COX-1 and COX-2 in different myeloma cell lines has received little attention [17] and it is valuable any investigation aimed at deepening the COXs link with MM. For this purpose, two cell lines derived of human multiple myeloma (NCI-H929 and RPMI-8226) were chosen for further investigations. NCI-H929 expresses only COX-1 in a very low percentage which was quantified as 9% with respect to HEK-293 COX-1, whereas RPMI-8226 does not express both COX-1 and COX-2 (Fig. 8). The engineered cell lines HEK-293 COX-1 and HEK-293 COX-2 that express COX-1 or COX-2, respectively, upon stimulation with 10 mg/mL tetracycline, have been used as positive controls [43].

Cytotoxic activity. Since no data regarding COX-1 inhibitors in MM treatment are available, 1 and 22, as two potent and selective COX-1 inhibitors, were tested in two MM NCI-H929 and RPMI 8226 cell lines to verify their cytotoxicity, alone and in combination with bortezomib, a commonly drug used in therapy. The effect on cell viability of 1 and 22 was compared with the effect of aspirin used alone and in combination with bortezomib.

Table 2
[a] Evaluation of 1 and 22 (100 mM) in in vitro coagulation of human plasma (n ¼ 3) by activated partial thromboplastin time (APTT) and prothrombin time (PT).

Compounds	PT (seconds) ± SD	APTT (seconds) ± SD
Ce	13.9 ± 0.8	44.8 ± 1.5
Cþ	300 ± 0.0	300 ± 0.0
1	14.2 ± 0.3	50.8 ± 0.23
22	13.7 ± 0.5	51.2 ± 0.3
aspirin	14.6 ± 1.0	50.3 ± 0.3

[a] Negative control (C-): 1% DMSO; positive control (Cþ): 100 mM rivaroxaban; 100 mM aspirin. The APTT and PT values are expressed by mean (n ¼ 3) and standard deviation (SD).

Table 3
[a] Hemolytic profile of 1 and 22 (100 mM) by hemolysis assay: values below 10% are considered non-hemolytic.

Compounds	Hemolysis (%) ± SD
Ce	0.00 ± 0.22
Cþ	100 ± 2.01
1	0.00 ± 0.02
22	0.0 ± 0.01
aspirin	0.0 ± 0.04

[a] 1% DMSO is the negative control (C-) and 1% Triton X-100 (Cþ) is the positive control; 100 mM aspirin. The hemolysis assay values are expressed by mean (n ¼ 3) and standard deviation (SD).

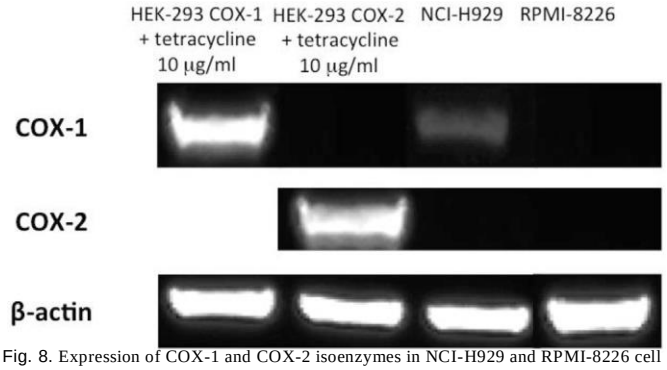

Fig. 8. Expression of COX-1 and COX-2 isoenzymes in NCI-H929 and RPMI-8226 cell lines [cell homogenates (30 mg protein) were applied to western blotting]. HEK-293 COX-1 and HEK-293 COX-2 were used as positive controls for COX-1 and COX-2 expression, respectively. The protein level of b-actin was used as loading control. The image is representative of one out of three experiments.

1, 22 and bortezomib were preliminarily used at different concentrations chosen upon their previously determined COXs EC_{50} or IC_{50} values. In both cell lines bortezomib was effective at very low concentrations (2 nM in NCI-H929 and 3 nM in RPMI-8226), whereas 1 and 22 were not cytotoxic at the concentrations used. 7.9 nM for compound 1, 42 nM for compound 22 and 1.7 mM for aspirin (COX-1 IC_{50}). In both RPMI 8226 and NCI-H929 cell lines the antiproliferative activity of bortezomib was not affected by the combined treatment with 1, 22 or aspirin (Fig. 9A and B).

In RPMI-8226, that does not express COXs, bortezomib has a 53% cytotoxicity whereas aspirin, 1 and 22 have a lower toxicity of 7, 1 and 4%, respectively. The cytotoxicity of the proteasome inhibitor bortezomib does not change when administered in association with the COX-1 inhibitors. In fact, its toxicity extent reaches 66% if co-administered with aspirin, 56% and 66% in co-administration with 1 or 22, respectively.

When the same experiment was performed with NCI-H929, that expresses only COX-1, the percentages changed. In all cases, co-administration leads to a decrease in the cytotoxicity of bortezomib compared to when it is administered alone.

These data demonstrate that, in our conditions, no-synergistic cytotoxic effect was observed by the co-administration of bortezomib with aspirin [22] and with other COX-1 inhibitors as in the case of 1 and 22.

Cell cycle analysis. Cytofluorimetric analysis of NCI-H929 and RPMI-8226 cell cycle was performed to evaluate the effects of bortezomib alone or in combination with COX-1 inhibitors 1, 22 and aspirin on cellular cycle. Cells were treated for 48 h with different concentrations 1, 22 or aspirin, chosen based on their IC_{50} or EC_{50} values from cytostatic effect. In NCI-H929, bortezomib alone displayed 10% more cells in G0/G1 and S cell cycle phases compared to control cells, while bortezomib in combination with COX-1 inhibitors showed a higher alteration of the normal phases of the cycle (15% more cells were registered in G0/G1 and S cell cycle phases) compared to control and bortezomib treated cells (Fig. 10).

Interestingly, in RPMI-8226 cells no difference was detected between treated cells and control cells (data not shown), while by treating NCI-H929 with bortezomib, aspirin, 1 and 22 most of the cells are in phase G2/M like the control, while co-administration of bortezomib with all COX-1 inhibitors seems to have an effect on the cell cycle. In fact, a reduction in the number of cells in G2 phase in favor of G0/G1 and S phases is detected.

Apoptosis. The apoptotic effect exerted by bortezomib alone or in combination with COX-1 inhibitors were determined using Annexin V/PI in NCI-H929 and RPMI-8226 cells. In NCI-H929 no apoptosis was detected after treatment with COX-1 inhibitors (Annexin V/PI negative), while 50% of cells were registered in an early apoptotic phase after treatment with bortezomib (Annexin V positive/PI negative). There is a significant shift of cells treated with bortezomib in combination with compound 1, 22 or aspirin from Annexin V positive/PI negative quadrant (early apoptotic cells) compared to control cells (Fig. 11).

In NCI-H929 cell line, cells in apoptotic phase are 49% when treated with bortezomib. Their percentage increases to 64, 61 and 55 when co-administered with 1, 22 and aspirin, respectively.

In RPMI-8226 cells with bortezomib alone or in combination with COX inhibitors displayed an apoptotic effect not so different from the control cells, with only 10% of cells detected in an early apoptotic phase (Annexin V positive/PI negative; Fig. 12).

These results encourage to deepen the role of COX-1 inhibition in apoptosis, since a marked difference is observed when treating RPMI-8226 or NCI-H929 cell line.

3. Conclusions

In conclusion, with this work differently substituted 3,4-diarylisoxazoles were prepared and tested against COX-1 and COX-2 isoenzymes. Based on the obtained results some key features have been identified useful to design new potent and selective COX-1 inhibitors. One of these moieties is the vinyl linked to the

Table 4
Mutagenic and genotoxic activity of 1 and 22 (500 mM) without metabolic activation.

Compound	Ames testS. typhimurium				SOS chromotestE. coli	
	TA97	TA98	TA100	TA102	PQ35	PQ37
1	e	e	e	e	e	e
22	e	e	e	e	e	e
4-NQO[a]	þ	þ	þ	þ	þ	þ
DMSO[b]	e	e	e	e	e	e
aspirin	e	e	e	e	e	e

a) 4-NQO was used as a positive control.
b) 1% DMSO was used as a negative control.

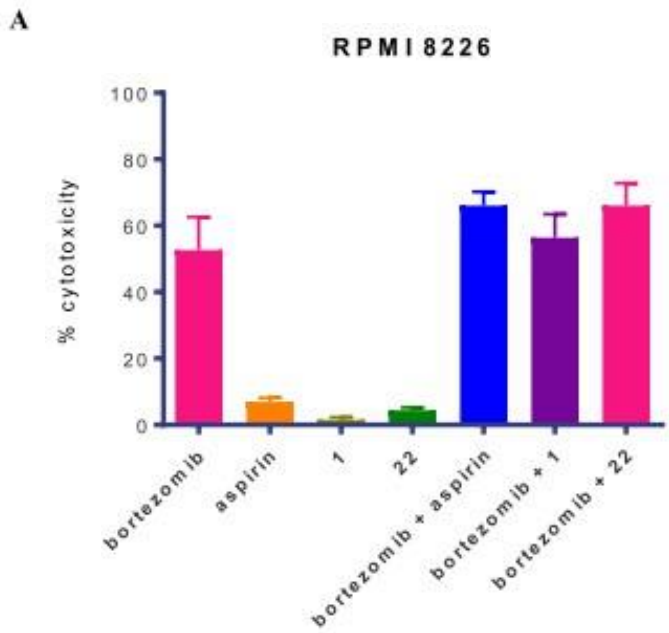

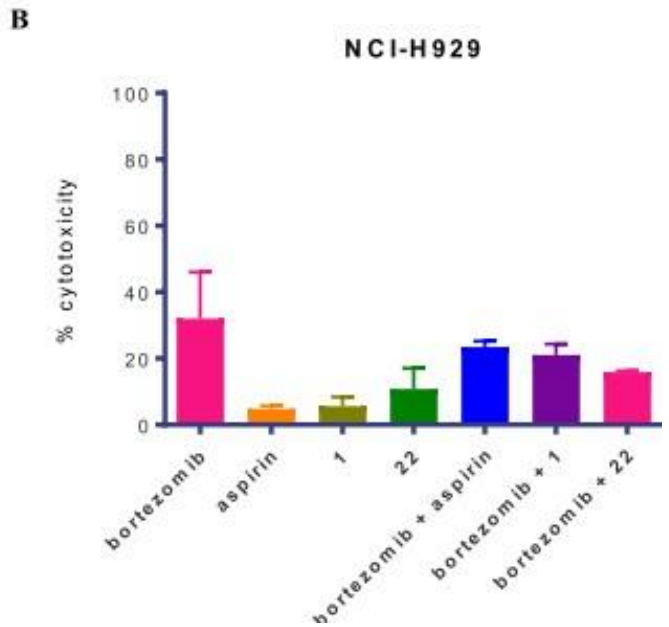

Fig. 9. Antiproliferative activity of bortezomib alone and in combination with 1, 22 or aspirin after 48h incubation time with RPMI-8226 (A) and NCI-H929 (B) cell lines. Error bars represent mean ± SD of three experiments in triplicate; one-way ANOVA followed by Bonferroni's post-hoc comparison test: $P > 0.05$.

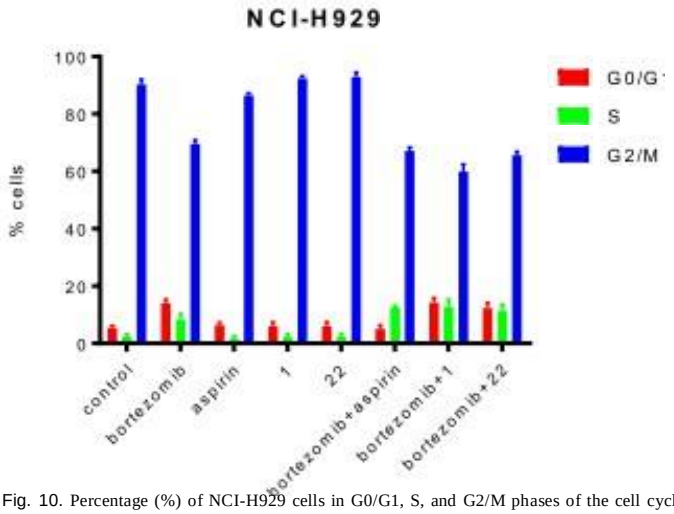

Fig. 10. Percentage (%) of NCI-H929 cells in G0/G1, S, and G2/M phases of the cell cycle during continuous exposure to different compounds concentrations: 7.9 nM for compound 1, 42 nM for compound 22 and 1.7 mM for aspirin (COX-1 IC_{50} values) and 2 nM for bortezomib (EC_{50} cytotoxic activity). Error bars represent mean ± SD of three experiments in triplicate; one-way ANOVA followed by Bonferroni's post-hoc comparison test: $P > 0.05$.

isoxazole-C5. It is detrimental the presence of an aminic group linked to phenyl present on the isoxazole-C3 but it is useful if the same p-$NH_2C_6H_4$ is linked to the isoxazole-C4 or a NH_2 is directly linked to the isoxzole-C5.

Among all newly synthesized compounds, 22 was found to be the most potent and selective COX-1 inhibitor (selectivity index in favor of COX-1 equal to 1190). The different disposition of 22 into COX-1 active site explains its lower potency than 1 (mofezolac). Compounds 1 and 22 were tested to verify their cytotoxic activity alone and in co-administration with bortezomib. They do not induce any change in bortezomib cytotoxic effect.

1 and 22 have a safety profile, as demonstrated by hemolysis assays and genotoxicity test, showing no hemolytic profile and nor mutagenic properties, respectively. Moreover, they efficiently inhibit platelet aggregation without affecting the coagulation cascade. A variety of results obtained by analyzing the effects of COX-1 inhibitors on cytotoxicity, cell cycle and apoptosis in two different cell lines (RPMI-8226 and NCI-H929) with a different COX expression profile prompt us to further investigate the role of COX-1 inhibition in multiple myeloma.

4. Experimental section

General methods. Melting points taken on electrothermal apparatus were uncorrected. ^{1}H NMR and ^{13}C NMR spectra were recorded on a Varian-Mercury 300 MHz, on a Varian-Inova 400 MHz spectrometer, on a Bruker-Aspect 3000 console 500 MHz spectrometer or on a Bruker Avance 600 MHz spectrometer and chemical shifts are reported in parts per million (d). ^{19}F NMR spectra were recorded by using $CFCl_3$ as internal standard. Absolute values of the coupling constant are reported. KBr pallet were prepared to record FT-IR spectra on a Perkin-Elmer 681 spectrometer. GC analyses were performed by using an HP1 column (methyl siloxane; 30m, 0.32 mm, 0.25 mm film thickness) on an HP 6890 model, Series II. Thin-layer chromatography (TLC) was performed on silica gel sheets with fluorescent indicator, the spots on the TLC were observed under ultraviolet light or were visualized by I_2 vapor exposure. Column chromatography was conducted by using silica gel 60 with a particle size distribution 40e63 mm and 230e400 ASTM. GC-MS analyses were performed on an HP 5995C model. MS-ESI analyses were performed on Agilent 1100 LC/MSD trap system VL. All synthesized compounds were analyzed by HPLC analysis, by an Agilent 1260 Infinity instrument equipped with a 1260 DAD VL þ detector on a column Poroshell 120 EC-18 3.0 50 mm 2.7 mm (eluent CH_3CN/H_2O ¼ 70/30; l¼ 280 nm), and their purity was found to be higher than 95%.

Materials. Tetrahydrofuran and dichloromethane from commercial source were purified by distillation (twice) from sodium wire or CaH_2, respectively, under nitrogen atmosphere. Commercially available dimethylformamide (DMF) was purified by distillation from CaH_2 under reduced pressure. 2.5 M n-BuLi in hexanes

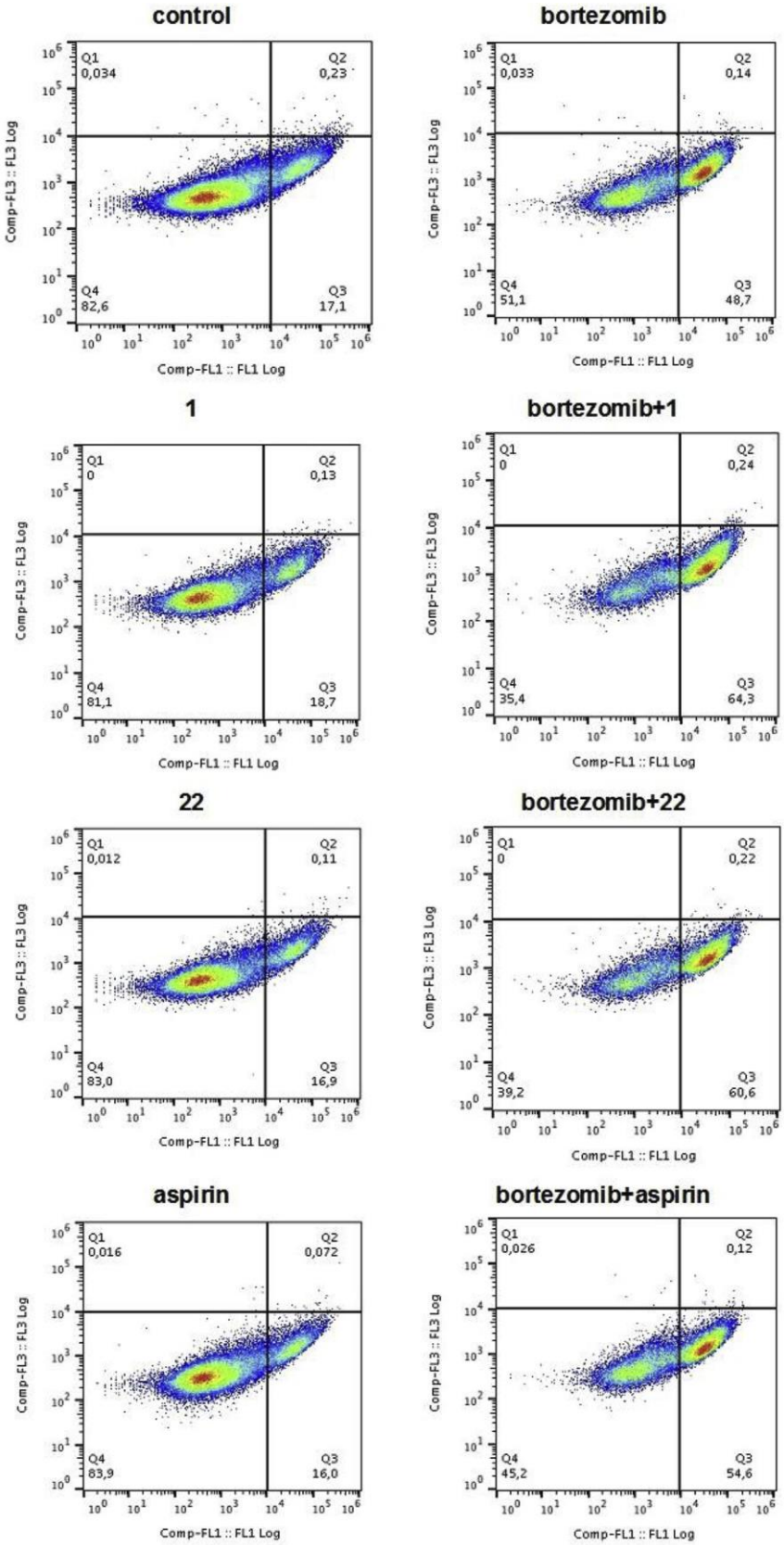

Fig. 11. Flow cytometry dot plot of NCI-H929 cells treated with the different tested compounds for 48 h at different concentrations: 7.9 nM, 42 nM, 1.7 mM and 2 nM for 1, 22, aspirin and bortezomib, respectively. The image is representative of one out of three experiments.

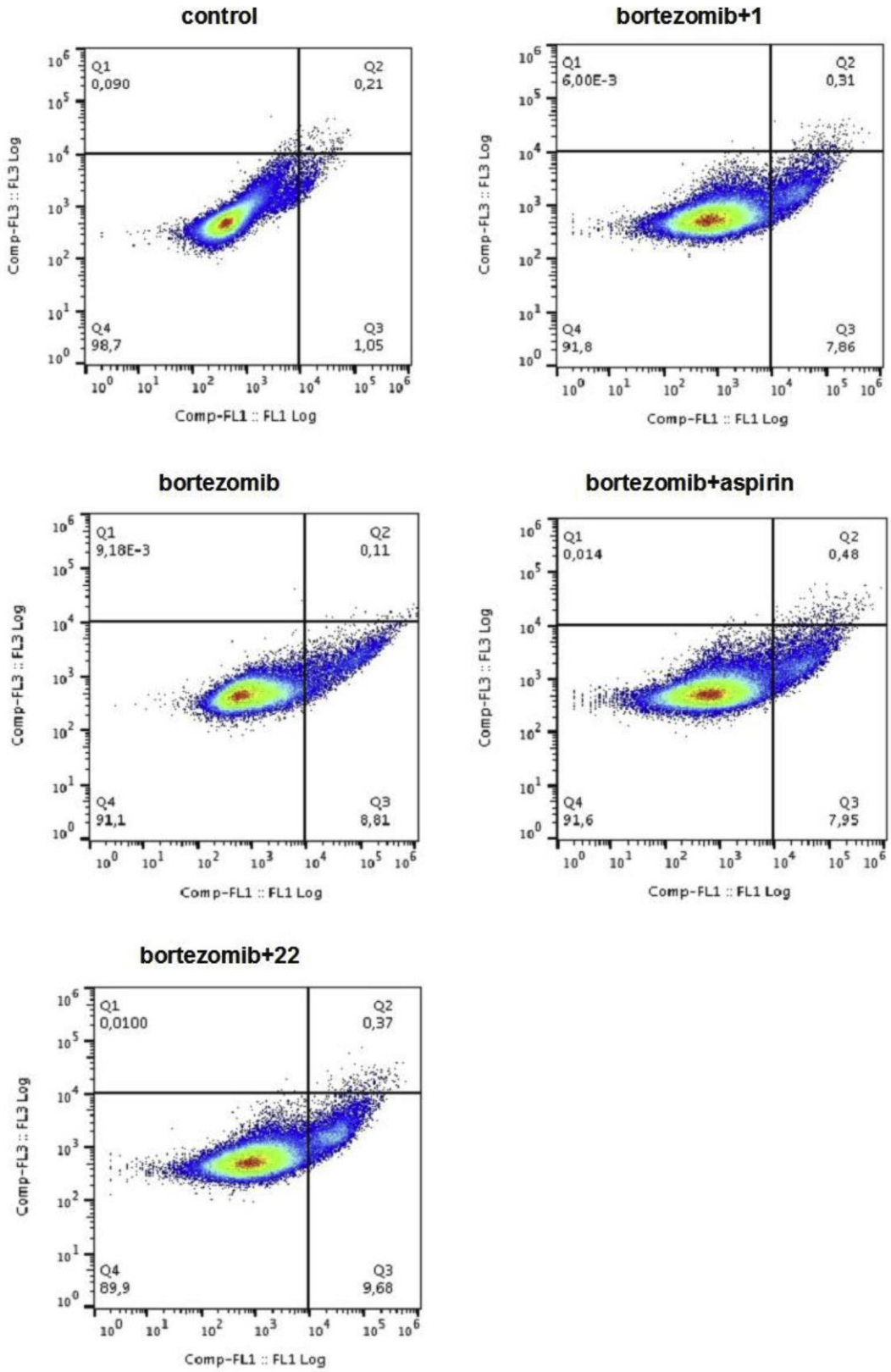

Fig. 12. Flow cytometry dot plot of RPMI-8226 cells treated with different tested compounds for 48 h at different concentrations: 7.9 nM, 42 nM, 1.7 mM and 2 nM for 1, 22, aspirin and bortezomib, respectively. The image is representative of one out of three experiments.

was purchased from Aldrich Chemical Co. and its titration was performed with N-pivaloyl-o-toluidine. Diisopropylamine from commercial source was purified by distillation from CaH_2 under reduced pressure and nitrogen atmosphere. All other chemicals and solvents were commercial grade further purified by distillation or crystallization prior to use.

Arylnitrile oxides (6a-c and 6e) were prepared from aldehydes through their conversion into the corresponding oximes (4a-c and 4e) and then into benzohydroximinoyl chlorides (5a-c and 5e) [44,45]. These were finally converted into nitrile oxides by treatment with Et_3N, followed by vacuum filtration of the formed $Et_3N^{\$}HCl$ from the solution. The so obtained arylnitrile oxide clear solution was immediately used in the cycloaddition reaction.

Oximes (4a-d), prepared from reaction of aldehydes/EtOH and $NH_2OH^{\$}HCl$/aq.NaOH, had analytical and spectroscopic data identical to those previously reported or commercially available.

4-Methoxybenzaldehyde oxime (4a). 90% yields. ^1H NMR (300 MHz, $CDCl_3$, d): 8.12 (s, 1H, CH); 7.54e6.91 (m, 4H, aromatic protons); 3.89e3.82 (bs, 1H, OH: exchanges with D_2O); 3.85 (s, 3H, CH_3).

4-Nitrobenzaldehyde oxime (4b). 97% yield.^1H NMR (300 MHz, $CDCl_3$, d): 8.20 (s, 1H, CH); 7.95e7.89 (bs, 1H, OH: exchanges with D_2O); 8.28e7.72 (m, 4H, aromatic protons).

4-Fluorobenzaldehyde oxime (4c). (80% yield). ^1H NMR (300 MHz, $CDCl_3$, d): 8.13 (s, 1H, CH); 8.02e7.97 (bs, 1H, OH: exchanges with D_2O); 7.59e7.07 (m, 4H, aromatic protons).

Synthesis of 4-(methylsulfonyl) benzaldehyde oxime (4e). First 4-(methylthio)benzaldehyde oxime (4d) was prepared in 88% yield according to the previous reported condition: ^1H NMR (600 MHz, $CDCl_3$, d): 8.50e7.80 (bs, 1H, OH: exchanges with D_2O); 8.10 (s,1H, CH); 7.49e7.47 (m, 2H, aromatic protons); 7.25e7.23 (m, 2H, aromatic protons); 2.50 (s, 3H, CH_3);^{13}C NMR (125 MHz, $CDCl_3$, d): 149.8, 141.3, 128.5, 127.3, 126.1, 15.3. Then, in a round bottom flask 4-(methylthio)benzaldehyde oxime (13.6 mmol, 2.28 g) was dissolved in anhydrous DMF (23 mL) at 0 C by an ice bath. 0.5 N HCl (0.57 mL) was added to the reaction mixture kept at 0 C, and then Oxone® (39 mmol, 12 g) was added. The reaction mixture was allowed to reach room temperature in 1 h, until the disappearance of the oxime 4d. After the dilution with water, the reaction product was extracted three times with chloroform. The combined organic phases were washed with brine (3 x 15 mL), dried over anhydrous Na_2SO_4 and then the solvent distilled in vacuum. 4-(Methylsulfonyl)benzaldehyde oxime (4e) was isolated in 93% yield as a mixture of E and Z isomers:^1H NMR (600 MHz, $CDCl_3$, d): 8.60e8.50 (bs, 1H, OH: exchanges with D_2O, Z isomer); 8.18 (s, 1H, CH); 7.96e7.95 (m, 2H, aromatic protons); 7.85e7.75 (bs, 1H, OH: exchanges with D_2O, E isomer); 7.78e7.77 (m, 2H, aromatic protons); 3.08 (s, 3H, CH_3, Z isomer); 3.07 (s, 3H, CH_3 E isomer);^{13}C NMR (125 MHz, $CDCl_3$, both isomers, d): 148.6, 141.4, 128.0, 127.9, 127.7, 126.1, 44.5, 29.7.

Synthesis of benzohydroximinoyl chlorides (5a-c and 5e): general procedure. Each oxime (0.50 g, 4.50 mmol) was dissolved in anhydrous DMF (5 mL) in a round-bottom flask equipped with magnetic stirrer and cooled at 0 C. N-chlorosuccinimide (NCS) (0.60 g, 4.50 mmol) was slowly added, and the obtained suspension was stirred at room temperature. When the reaction was completed, Et_2O was added and the solution was washed with water until the removal of DMF. The combined organic extracts were dried over anhydrous Na_2SO_4, and the solvent was distilled in vacuum.

N-Hydroxy-4-methoxybenzimidoyl chloride (5a). 91% yield. ^1H NMR (600 MHz, $CDCl_3$, d): 8.20e8.15 (bs, 1H, OH: exchanges with D_2O); 7.80e6.91 (m, 4H, aromatic protons); 3.85 (s, 3H, CH_3). NMR data are in agreement with those previously reported [46,47].

N-Hydroxy-4-nitrobenzimidoyl chloride (5b). 95% yield.^1H NMR (600 MHz, $CDCl_3$, d): 8.40-8.35 (bs, 1H, OH: exchanges with D_2O); 8.28e8.04 (m, 4H, aromatic protons). NMR data are in agreement with those previously reported [48].

N-Hydroxy-4-fluorobenzimidoyl chloride (5c). 76% yield.^1H NMR (600 MHz, $CDCl_3$, d): 8.26e8.18 (bs, 1H, OH: exchanges with D_2O); 7.85e7.09 (m, 4H, aromatic protons). NMR data are in agreement with those previously reported [46,47].

N-Hydroxy-4-(methylsulfonyl)benzimidoyl chloride (5e). 85% yield.^1H NMR (600 MHz, $CDCl_3$, d): 12.85e12.80 (bs, 1H, OH: exchange with D_2O); 8.05e8.00 (m, 4H, aromatic protons); 3.25 (s, 3H, CH_3).

Synthesis of 3,4-diarylisoxazoles (8-12): general procedure [49]. The commercially available 3-aryl-2-propanone (7) (0.6 mmol) was dropwise added to a suspension of NaH (95% w/w, 1.2 mmol) in anydrous THF (6 mL) kept at 0 C under nitrogen atmosphere, using a nitrogen-flushed, three necked flask equipped with a magnetic stirrer, a nitrogen inlet and a dropping funnel. After the yellow mixture was stirred for 1 h, a limpid solution of the arylnitrile oxide (6a-c and 6e) (0.6 mmol) in anydrous THF (3 mL) was added. The reaction mixture was allowed to reach room temperature, stirred overnight and then quenched by adding aqueous NH_4Cl solution. The reaction products were extracted three times with ethyl acetate. The combined organic phases were dried over anhydrous Na_2SO_4 and then the solvent distilled in vacuum. Column chromatography (silica gel, petroleum ether: ethyl acetate ¼ 8/2) of the residue affords the 3,4-diaryl-5-methylisoxazole (8-12) in 50e91% yields.

3,4-Bis(4-methoxyphenyl)-5-methylisoxazole (8). 50% yield. Mp 95e98 C (EtOH), light yellow powder.^1H NMR (300 MHz, $CDCl_3$, d): 7.37 (d, 2H, J ¼ 9.0 Hz, aromatic protons); 7.09 (d, 2H, J ¼ 9.0 Hz, aromatic protons); 6.90 (d, 2H, J ¼ 9.0 Hz, aromatic protons); 6.83 (d, 2H, J ¼ 9.0 Hz, aromatic protons); 3.80 (s, 3H, OCH_3); 3.83 (s, 3H, OCH_3); 2.40 (s, 3H, CH_2).

4-(4-Fluorophenyl)-5-methyl-3-(4-nitrophenyl)isoxazole (9). 60% yield. Mp 110e113 C (Et_2O), yellow crystals. FT-IR (KBr): 3072, 2917, 2849, 1629, 1594, 1519, 1506, 1452, 1432, 1398, 1349, 1326, 1290, 1239, 1221, 1158, 1108, 1092, 1028, 1013, 979, 963, 926, 863, 846, 814, 764, 752, 727, 714, 689 cm^{1}.^1H NMR (600 MHz, $CDCl_3$, d): 8.21e8.18 (m, 2H, aromatic protons); 7.63e7.61 (m, 2H, aromatic protons); 7.15e7.12 (m, 4H, aromatic protons); 2.47 (s, 3H, CH_3).^{13}C NMR (150 MHz, $CDCl_3$, d): 167.7, 162.6 (d,$^1J_{19F\text{-}13C}$ ¼ 249 Hz), 159.2, 148.4, 135.4, 131.5 (d, $^3J_{19F\text{-}13C}$ ¼ 8 Hz), 129.2, 125.5 (d, $^4J_{19F\text{-}13C}$ ¼ 4 Hz), 123.8, 116.2 (d,$^2J_{19F\text{-}13C}$ ¼ 22 Hz), 115.1, 11.5.^{19}F NMR (470 MHz, $CDCl_3$, d): 112.8 (m). HRMS (ESI-TOF) m/z: [M þ Na]^{þ} Calcd for $C_{16}H_{11}FN_2O_3Na$: 321.2771; Found 321.2767.

3-(4-Fluorophenyl)-4-(4-methoxyphenyl)-5-methylisoxazole (10). 50% yield. Mp 93e95 C, white solid. FT-IR (KBr): 3010, 2963, 2933, 2834, 1634, 1606, 1574, 1509, 1431, 1374, 1306, 1290, 1225, 1175, 1160, 1105, 1039, 1022, 962, 909, 815, 747, 707, 578, 561 cm^{1}.^1H NMR (600 MHz, $CDCl_3$, d): 7.46e7.43 (m, 2H, p-F-Ar: aromatic protons); 7.10e7.08 (m, 2H, aromatic protons); 7.03e6.98 (m, 2H, p-F-Ar: aromatic protons); 6.94e6.91 (m, 2H, aromatic protons); 3.85 (s, 3H, OCH_3); 2.43 (s, 3H, CH_3).^{13}C NMR (150 MHz, $CDCl_3$, d): 166.5, 163.4 (d,$^1J_{19F\text{-}13C}$ ¼ 248 Hz), 160.3, 159.2, 131.0, 130.3 (d,$^3J_{19F\text{-}13C}$ ¼ 8 Hz), 122.3, 115.6 (d,$^2J_{19F\text{-}13C}$ ¼ 22 Hz), 114.3, 55.3, 11.5.^{19}F NMR (470 MHz, $CDCl_3$, d): 111.6 (m). HRMS (ESI-TOF) m/z: [M þ Na]^{þ} Calcd for $C_{17}H_{14}FNO_2Na$: 306.3052; Found 305.3057.

4-(4-Fluorophenyl)-5-methyl-3-[4-(methylsulfonyl)phenyl] isoxazole (11). 91% yield. Mp 152e154 C, pale yellow powder. FT-IR (KBr): 3074, 2920, 2850, 1629, 1599, 1568, 1513, 1458, 1434, 1391, 1313, 1237, 1221, 1154, 1121, 1092, 1015, 956, 911, 843, 779, 606 cm^{1}.^1H NMR (600 MHz, $CDCl_3$, d): 7.91 (d, J ¼ 8.8 Hz, 2H, aromatic protons); 7.63 (d, J ¼ 8.8 Hz, 2H, aromatic protons); 7.16e7.10 (m, 4H, aromatic protons); 3.07 (s, 3H, SO_2CH_3); 2.47 (s, 3H, CH_3).

^{13}C NMR (150 MHz, $CDCl_3$, δ): 167.6, 162.5 (d, $^1J_{19F\text{-}13C}$ ¼ 248 Hz), 159.5, 148.2, 134.5, 131.5 (d, $^3J_{19F\text{-}13C}$ ¼ 8 Hz), 129.2, 125.5 (d, $^4J_{19F\text{-}13C}$ ¼ 4 Hz), 116.2 (d, $^2J_{19F\text{-}13C}$ ¼ 22 Hz), 44.4, 11.5. ^{19}F NMR (470 MHz, $CDCl_3$, δ): 113,5 (m). GC-MS (70 eV) m/z (rel. int.): 331 [M^+,100], 316 (10), 289 (79), 210 (29), 209 (19), 208 (20), 183 (12), 122 (25), 121 (18), 107 (45), 96 (11), 43 (45). HRMS (ESI-TOF) m/z: [M + Na]$^+$ Calcd for $C_{17}H_{14}FNO_3SNa$: 354.0571; Found 354.0567.

4-(4-Methoxyphenyl)-5-methyl-3-(4-nitrophenyl)isoxazole (12). 76% yield. Mp 132–134 C (Et_2O), white powder. FT-IR (KBr): 3072, 3036, 3012, 2970, 2940, 2925, 2845, 1628, 1600, 1573, 1520, 1435, 1345, 1290, 1248, 1177, 1107, 1039, 1020, 962, 918, 862, 835, 728, 716, 608 cm^{-1}. ^{1}H NMR (600 MHz, $CDCl_3$, δ): 8.19–8.17 (m, 2H, aromatic protons); 7.66–7.64 (m, 2H, aromatic protons); 7.10–7.08 (m, 2H, aromatic protons); 6.95–6.93 (m, 2H, aromatic protons); 3.86 (s, 3H, OCH_3); 2.46 (s, 3H, CH_3). ^{13}C NMR (150 MHz, $CDCl_3$, δ): 167.4, 159.5, 159.3, 148.3, 135.7, 130.9, 129.2, 123.7, 121.5, 115.6, 114.5, 114.5, 55.3, 11.5. GC-MS (70 eV) m/z (rel. int.): 310 [M^+, 100], 295 (8), 268 (17), 253 (7), 134 (24), 119 (24), 91 (9), 76 (5), 43 (6). HRMS (ESI-TOF) m/z: [M + Na]$^+$ Calcd for $C_{17}H_{14}N_2O_4Na$: 333.3112; Found 333.3117.

Synthesis of 3-(4-aminophenyl)-4-(4-methoxyphenyl)-5-methylisoxazole (13). To a stirred mixture of stannous chloride (782 mg, 3.46 mmol) in hydrochloric acid 37% (2.8 mL) at 25 C, a solution of 4-(4-methoxyphenyl)-3-(4-nitrophenyl)isoxazol-5-amine (12) (165 mg, 0.495 mmol) dissolved in absolute EtOH (8 mL) was added. The reaction mixture was kept under reflux for 24 h. Then,10% NaOH (10 mL) was added to the reaction mixture till pH ¼ 12, and the aqueous phase extracted three times with dichloromethane. The combined organic extracts were dried over anhydrous Na_2SO_4 and the solvent distilled in vacuum. The residue afforded the product with 45% yield. Mp 152–153 C (Et_2O), white powder. FT-IR (KBr): 3473, 3355, 3225, 3008, 2959, 2932, 1634, 1608, 1514, 1435,1406, 1369, 1302, 1288, 1250, 1173, 1104, 1042, 1024, 900, 838, 749, 636, 619 cm^{-1}. ^{1}H NMR (500 MHz, $CDCl_3$, δ): 7.27–7.24 (m, 2H, aromatic protons); 7.13–7.10 (m, 2H, aromatic protons); 6.92–6.90 (m, 2H, aromatic protons); 6.61–6.59 (m, 2H, aromatic protons); 3.84 (s, 3H, OCH_3); 3.90–3.75 (bs, 2H, NH_2: exchanges with D_2O); 2.40 (s, 3H, CH_3). ^{13}C NMR (150 MHz, $CDCl_3$, δ): 165.9, 161.0, 159.0, 147.4, 131.0, 129.6, 123.0, 119.2, 115.0, 114.7, 114.1, 55.3, 11.5. HRMS (ESI-TOF) m/z: [M + Na]$^+$ Calcd for $C_{15}H_{12}FN_3ONa$: 303.3291; Found 303.3291.

Synthesis of 3-(4-acetamidophenyl)-4-(4-methoxyphenyl)-5-methylisoxazole (14). 3-(4-Aminophenyl)-4-(4-methoxyphenyl)-5-methylisoxazole (13) (330 mg, 1.2 mmol) in acetic anhydride (1.12 mL, 12 mmol) and pyridine (0.44 mL) was stirred at room temperature for 16 h. Then, the reaction mixture was added with sat. aq. $NaHCO_3$ and the product extracted with EtOAc (three times). The combined organic phases were dried with anhydrous Na_2SO_4, filtered and the solvent distilled under reduced pressure. **14** was obtained in quantitative yield as a white solid and used to prepare **16** without any further purification. FT-IR (KBr): 3345, 2956, 2919, 2849, 1670, 1606, 1536, 1514, 1462, 1369, 1316, 1288, 1253, 1178, 1106, 1024, 1004, 956, 893, 839, 814, 797, 750, 682 cm^{-1}. ^{1}H NMR (600 MHz, $CDCl_3$, δ): 8.00–7.92 (bs, 1H, NH: exchanges with D_2O); 7.46–7.45 (m, 2H, aromatic protons); 7.37–7.36 (m, 2H, aromatic protons); 7.08–7.06 (m, 2H, aromatic protons); 6.90–6.88 (m, 2H, aromatic protons); 3.82 (s, 3H, OCH_3); 2.40 (s, 3H, CH_3), 2.14 (s, 3H, CH_3). ^{13}C NMR: (750 MHz, $CDCl_3$, δ): 163.6, 161.6, 155.8, 154.4, 134,1, 126.2, 124.3, 120.2, 117.6, 114.7, 110.5, 109.5, 50.5, 24.9, 19.9. HRMS (ESI-TOF) m/z: [M + Na]$^+$ Calcd for $C_{19}H_{18}N_2O_3Na$: 345.3663; Found 345.3664.

Synthesis of 3,4-diarylisoxazol-5-acetic acids (1, 15–17): general procedure. 1.6 N n-BuLi (5 mL) was dropwise added to a stirred solution of 3,4-diaryl-5-methylisoxazole (2.0 g, 7.0 mmol) in THF (30 mL) kept at −78 C under an argon atmosphere. After 1h, anhydrous gaseous CO_2 was bubbled into the stirred red colored reaction mixture, till the color disappearance. Then, the yellow stirred reaction mixture was allowed to warm to room temperature, and concentrated under reduced pressure, after the addition of 3N HCl (5 mL). The aqueous solution was extracted twice with EtOAc, and the combined organic extracts were dried over anhydrous Na_2SO_4, filtered and the solvent distilled under reduced pressure. The obtained sticky foam residue was recrystallized from methanol to give the 3,4-diarylisoxazol-5-acetic acids as solid substances (50–71% yields).

2-[3-(4-Fluorophenyl)-4-(4-methoxyphenyl)isoxazol-5-yl] acetic acid (15). 50% yield. Mp 93–95 C, white solid. FT-IR (KBr): 3468–2963, 2933, 2834, 1634, 1606, 1574, 1509, 1431, 1374, 1306, 1290, 1225, 1175, 1160, 1105, 1039, 1022, 962, 909, 815, 747, 707 cm^{-1}. ^{1}H NMR (600 MHz, $CDCl_3$, δ): 7.48–7.45 (m, 2H, p-F-aromatic protons); 7.15–7.14 (m, 2H, aromatic protons); 7.04–7.01 (m, 2H, p-F-aromatic protons); 6.95–6.93 (m, 2H, aromatic protons); 3.86 (s, 3H, OCH_3); 3.84 (s, 2H, CH_2). ^{13}C NMR (150 MHz, $CDCl_3$, δ): 166.5, 163.4 (d, $^1J_{19F\text{-}13C}$ ¼ 248 Hz), 160.3, 159.2, 131.0, 130.3 (d, $^3J_{19F\text{-}13C}$ ¼ 8 Hz), 122.3, 115.6 (d, $^2J_{19F\text{-}13C}$ ¼ 22 Hz), 114.3, 55.3, 11.5. ^{19}F NMR (470 MHz, $CDCl_3$, δ): 111.6 (m). HRMS (ESI-TOF) m/z: [M + Na]$^+$ Calcd for $C_{18}H_{14}FNO_4Na$: 350.3065; Found 350.3057.

2-[3-(4-Aminophenyl)-4-(4-methoxyphenyl)isoxazol-5-yl] acetic acid (16). Mp 206–209 C. FT-IR (KBr): 3423–3000, 2957, 2939, 1635, 1606, 1515, 1463, 1342, 1410, 1342, 1300, 1242, 1159, 1098, 1037 cm^{-1}. ^{1}H NMR (500 MHz, $CDCl_3$, δ): 7.26–7.24 (m, 2H, aromatic protons); 7.17–7.13 (m, 2H, aromatic protons); 6.93–6.90 (m, 2H, aromatic protons); 6.60–6.58 (m, 2H, aromatic protons); 6.50–6.40 (bs, 2H, NH_2: exchange with D_2O); 3.83 (s, 3H, OCH_3); 3.79 (s, 2H, CH_2). ^{13}C NMR (125 MHz, $CDCl_3$, δ): 169.2, 158.5, 158.4, 156.8, 145.0, 128.5, 127.0, 119.2, 116.1, 115.1, 112.2, 111.7, 52.7, 27.1 HRMS (ESI-TOF) m/z: [M + H]$^+$ Calcd for $C_{18}H_{16}N_2O_4$ 323.1110; Found 323.1109.

2-[3-(4-Acetamidophenyl)-4-(4-methoxyphenyl)isoxazol-5-yl]acetic acid (17). Mp 84–87 C. FT-IR (KBr): 3312–3050, 2958, 2929, 2848, 1724, 1677, 1602, 1529, 1431, 1318, 1294, 1249, 1178, 1020, 836, 611 cm^{-1}. ^{1}H NMR (600 MHz, CD_3OD, δ): 7.55–7.54 (m, 2H, aromatic protons); 7.37–7.36 (m, 2H, aromatic protons); 7.17–7.16 (m, 2H, aromatic protons); 6.98–6.96 (m, 2H, aromatic protons); 3.83 (s, 3H, OCH_3); 3.79 (s, 2H, CH_2), 2.13 (s, 3H, $COCH_3$); ^{13}C NMR (125 MHz, CD_3OD, δ): 170.3, 170.0, 163.2, 160.7, 159.8, 139.9, 130.8, 128.5, 124.1, 121.3, 119.4, 117.3, 114.0, 54.3, 31.1, 22.5. HRMS (ESI-TOF) m/z: [M - H]$^-$ Calcd for $C_{20}H_{18}N_2O_5$ 365.1137; Found 365.1135.

Synthesis of 5-bromomethyl-3,4-bis(4-methoxyphenyl)isoxazole (18). To a solution of 3,4-bis(4-methoxyphenyl)-5-methylisoxazole, **8** (500 mg, 1.7 mmol) in CCl_4 (8.75 mL) kept at room temperature, NBS (362 mg, 2.05 mmol), and AIBN (140 mg, 0,85 mmol) were added. The mixture was stirred overnight at room temperature, giving a pale-yellow homogeneous solution. After 16 h the same quantities of NBS and AIBN were added. The mixture was refluxed for further 2 h and then the reaction was stopped by addition of distilled water. The aqueous solution was extracted with CH_2Cl_2. The organic layer was dried over anhydrous sodium sulfate, filtered and the solvent distilled under reduced pressure. After flash chromatography on silica gel (hexane/ethyl acetate 9:1) of the reaction crude, the product was isolated as a yellow semi-solid with 55% yield. ^{1}H NMR (400 MHz, $CDCl_3$, δ): 7.38 (d, 2H, J ¼ 8.8 Hz, aromatic protons); 7.20 (d, 2H, J ¼ 8.8 Hz, ArH); 6.94 (d, 2H, J ¼ 8.8 Hz, aromatic protons); 6.84 (d, 2H, J ¼ 8.8 Hz, aromatic protons); 4.44 (s, 2H, CH_2); 3.84 (s, 3H, CH_3); 3.80 (s, 3H, CH_3). GC-MS (70 eV) m/z (rel. int.): 375 [M^+ (Br^{81}), (59)], 373 [M^+ (Br^{79}), (58)], 295 (83), 252 (100), 238 (28), 133 (35), 119 (37). HRMS (ESI-TOF) m/z: [M + Na]$^+$ Calcd for $C_{18}H_{16}BrNO_3Na$: 397.3312; Found 397.3315.

Synthesis of 5-fluoromethyl-3,4-bis(4-methoxyphenyl)isoxazole (19). To a powder of 5-bromomethyl-3,4-bis(4-methoxyphenyl)isoxazole (18) (50 mg, 0.134 mmol) kept at room temperature, anhydrous 1M TBAF (THF solution, 402 ml) was added dropwise, and the mixture was stirred for 24 h at room temperature to give a pale red homogeneous solution. The reaction was stopped by addition of distilled water and the aqueous solution was extracted with ethyl acetate. The organic layer was dried over anhydrous sodium sulfate, filtered and the solvent distilled under reduced pressure. After column chromatography on silica gel (hexane/ethyl acetate 8:2) of the reaction crude, the product was isolated as a yellow solid (45% yield). Mp 118e120 C.^{1}H NMR (400 MHz, $CDCl_3$, d): 7.42e7.39 (d, 2H, J ¼ 9.0 Hz, aromatic protons). 7.18e7.15 (d, 2H, J ¼ 9.0 Hz, aromatic protons); 6.94e6.91 (d, 2H, J ¼ 9.0Hz, aromatic protons), 6.87e6.84 (d, 2H, J ¼ 9.0 Hz aromatic protons), 5.41e5.25 (d, 2H, J_{H-F} ¼ 48.41 Hz, CH_2), 3.84 (s, 3H, CH_3); 3.81 (s, 3H, CH_3). HRMS (ESI-TOF) m/z: [M þ Na]^þ Calcd for $C_{18}H_{16}FNO_3Na$: 336.3314; Found 336.3317.

Preparation of 3,4-bis(4-methoxyphenyl)-5-hydroxyethylisoxazole (20). To a solution of mofezolac (1) (200 mg, 0.589 mmol) in anhydrous THF (2 mL) kept at 0 C by an ice-bath, 1M BMS in THF (1.16 mL, 1.16 mmol) was added dropwise. The reaction mixture was stirred overnight at room temperature to give a pale yellow homogeneous solution. Distilled water (1 mL), 20% NaOH (1 mL) and 35% H_2O_2 (1 mL) were added and the obtained reaction mixture was stirred for 1 h. Then, the solution was extracted with ethyl acetate. The organic layer was dried over anhydrous Na_2SO_4 and the solvent distilled under reduced pressure. The product was isolated as a yellow oil (87% yield) by flash chromatography on silica gel (hexane/ethyl acetate ¼ 6:4) of the reaction crude. FT-IR (KBr): 3391, 1610, 1574, 1248, 1029, 835, 799 cm^{-1}.^{1}H NMR (400 MHz, $CDCl_3$, d): 7.39 (d, 2H, J ¼ 9.0 Hz, aromatic protons); 7.21 (d, 2H, J ¼ 9.0 Hz, aromatic protons); 6.95 (d, 2H, J ¼ 9.0 Hz, aromatic protons), 6.85 (d, 2H, J ¼ 9.0 Hz, aromatic protons), 4.26 (t, 2H, J ¼ 6.6 Hz, CH_2); 4.44 (t, 2H, J ¼ 6.6 Hz, CH_2), 3.85 (s, 3H, CH_3); 3.81 (s, 3H, CH_3). HRMS (ESI-TOF) m/z: [M þ Na]^þ Calcd for $C_{19}H_{19}NO_4Na$: 348.3652; Found 348.3655.

Synthesis of 2-[3,4-bis(4-methoxyphenyl)isoxazol-5-yl] ethyl-4-methylbenzenesulfonate (21). To a solution of 3,4-bis(4-methoxyphenyl)-5-hydroxyethylisoxazole (20) (160 mg, 0.492 mmol), in CH_2Cl_2 (11.4 mL) kept at 0 C by an ice-bath, p-toluensulphonic anhydride (544 mg, 1.67 mmol) and triethylamine (466 ml) were added. The reaction mixture was stirred overnight at room temperature to give a pale yellow homogeneous solution. Then, water was added to the reaction mixture and the aqueous solution was extracted with CH_2Cl_2. The organic layer was dried over anhydrous Na_2SO_4 and the solvent distilled under reduced pressure. The product was isolated as a yellow semi-solid (60% yield) by flash chromatography on silica gel (hexane/ethyl acetate ¼ 7:3) of the reaction crude.^{1}H NMR (400 MHz, $CDCl_3$, d): 7.69 (d, 2H, J ¼ 9.0 Hz, aromatic protons); 7.33 (d, 2H, J ¼ 9.0 Hz, aromatic protons); 7.30 (d, 2H, J ¼ 9.0 Hz, aromatic protons); 7.03 (d, 2H, J ¼ 9.0 Hz, aromatic protons); 6.88 (d, 2H, J ¼ 9.0 Hz, aromatic protons); 6.82 (d, 2H, J ¼ 9.0 Hz, aromatic protons); 4.30 (t, 2H, J ¼ 6.6 Hz, CH_2); 3.82 (s, 3H, CH_3); 3.78 (s, 3H, CH_3); 3.05 (t, 2H, J ¼ 6.6 Hz, CH_2); 2.36 (s, 3H, CH_3). HRMS (ESI-TOF) m/z: [M þ Na]^þ Calcd for $C_{26}H_{25}NO_6SNa$: 502.5483; Found 502.5485.

Synthesis of 3,4-bis(4-methoxyphenyl)-5-vinylisoxazole (22). To 21 (30 mg, 0.063 mmol) TBAF 1M in THF (188 mL) was added dropwise. The reaction mixture was stirred for 24 h at room temperature to give a pale yellow homogeneous solution. The reaction was stopped by adding distilled water and product extracted with ethyl acetate. The organic layer was dried over anhydrous Na_2SO_4 and the solvent removed under reduced pressure. The product 22 was isolated as a yellow solid (55% yield) by chromatography on silica gel (hexane/ethyl acetate 8:2) of the reaction crude. Mp 89e91 C.^{1}H NMR (600 MHz, $CDCl_3$, d): 7.39 (d, 2H, J ¼ 8.3 Hz, aromatic protons); 7.13 (d, 2H, J ¼ 8.3 Hz, aromatic protons); 6.92 (d, 2H, J ¼ 8.3 Hz, aromatic protons); 6.84 (d, 2H, J ¼ 8.3 Hz, aromatic protons); 6.52 (dd, 1H, J ¼ 11.5 and 17.6 Hz, vinyl proton); 6.10 (d, 1H, J ¼ 17.6 Hz, vinyl proton); 5.53 (d, 1H, J ¼ 11.3 Hz, vinyl proton). ^{13}C NMR (150 MHz, $CDCl_3$, d): 164.0, 161.1, 160.5, 159.3, 131.3, 129.7, 121.9, 121.6, 121.2, 120.0, 116.1, 114.2, 113.9, 55.3, 55.2, 29.7. GC-MS (70 eV) m/z (rel. int.): 307 [M^þ, 100], 252 (57), 221 (20), 160 (43),133 (24), 119 (35),102 (28). HRMS (ESI-TOF) m/z: [M þ Na]^þ Calcd for $C_{19}H_{19}NO_4Na$: 330.3508; Found 330.3509.

Synthesis of 3,4-diarylisoxazol-5-amines (23e26): general procedure. 2.5 M t-BuLi in pentane (1.8 mL, 3 mmol) was added to a solution of phenylacetonitrile (0.30 mL, 2.23 mmol) in anhydrous THF (10 mL) kept at 78 C under nitrogen atmosphere, using a nitrogen-flushed, three necked flask equipped with a magnetic stirrer, a nitrogen inlet and two dropping funnels. The reaction mixture was stirred for 1 h at 78 C, then the solution of arylnitrile oxide (2.23 mmol) in anhydrous THF (10 mL) was added. The obtained orange-colored reaction mixture was allowed to reach room temperature and stirred overnight. After quenching with aqueous NH_4Cl solution, the reaction products were extracted three times with ethyl acetate. The organic phase was dried over anhydrous Na_2SO_4 and then the solvent distilled in vacuum. Column chromatography (silica gel, petroleum ether/ethyl acetate ¼ from 7:3 to 6:4) of the residue affords 3,4-diarylisoxazol-5-ylamine in 30e59% yield.

3,4-Bis(4-methoxyphenyl)isoxazol-5-amine (23). 35% yield. Yellow oil. FT-IR (KBr): 3367, 3297, 2954, 2931, 2833, 1635, 1610, 1515, 1450, 1338, 1294, 1247, 1174, 1109, 1031 cm^{-1}.^{1}H NMR (500 MHz, $CDCl_3$, d): 7.39 (d, 2H, J ¼ 8.8 Hz, aromatic protons); 7.12 (d, 2H, J ¼ 8.8 Hz, aromatic protons); 6.90 (d, 2H, J ¼ 8.8 Hz, aromatic protons); 6.83 (d, 2H, J ¼ 8.8 Hz, aromatic protons); 4.46 (bs, NH_2: exchange with D_2O); 3.82 (s, 3H, CH_3); 3.80 (s, 3H, CH_3);^{13}C NMR (150 MHz, $CDCl_3$, d): 165.3, 161.5, 160.4, 158.6, 130.7, 129.9, 129.6, 129.4, 122.3, 127.8, 122.8, 121.9, 114.6, 114.5, 113.8, 93.8, 55.3, 55.2. GC-MS (70 eV) m/z (rel. int.): 296 [M^þ], 135 (100). HRMS (ESI-TOF) m/z: [M þ Na]^þ Calcd for $C_{17}H_{16}N_2O_3Na$: 319.3282; Found 319.3285.

3-(4-Fluorophenyl)-4-(4-methoxyphenyl)isoxazol-5-amine (24). 30% yield. Mp 184e187 C (EtOAc/hexane). FT-IR (KBr): 3423, 3291, 3264, 3165, 3078, 3000, 2957, 2939, 2911, 2835, 1638, 1606, 1515, 1463, 1342, 1410, 1342, 1300, 1285, 1242, 1220, 1179, 1159, 1037, 1022, 967, 902, 846, 834, 618 cm^{-1}.^{1}H NMR (600 MHz, $CDCl_3$, d): 7.47e7.45 (m, 2H, p-F-aromatic protons); 7.12e7.11 (m, 2H, aromatic protons); 7.03e7.00 (m, 2H, p-F-aromatic protons); 6.93e6.92 (m, 2H, aromatic protons); 4.55e4.50 (bs, NH_2: exchange with D_2O); 3.84 (s, 3H, OCH_3);^{13}C NMR (125 MHz, $CDCl_3$, d): 165.6, 163.4 (d, $^1J_{19F-13C}$ ¼ 249 Hz), 161.0, 158.8, 130.6, 130.1 (d, $^3J_{19F-13C}$ ¼ 8 Hz), 125.7 (d, $^4J_{19F-13C}$ ¼ 3 Hz), 122.4, 115.5 (d, $^2J_{19F-13C}$ ¼ 21 Hz), 114.6. GC-MS (70 eV) m/z (rel.int.): 284 [M^þ, 41], 269 (15), 268 (12), 256 (37), 241 (10), 170 (8), 135 (67), 134 (53), 123 (100), 122 (43), 121 (27), 119 (13), 107 (14), 94 (10), 77 (14), 75 (10), 65 (9). HRMS (ESI-TOF) m/z: [M þ Na]^þ Calcd for $C_{16}H_{13}FN_2O_2Na$: 307.2943; Found 307.2945.

4-(4-Fluorophenyl)-3-(4-nitrophenyl)isoxazol-5-amine (25). 59% yield. Mp 216e218 C (EtOAc/hexane). FT-IR (KBr): 3429, 3395, 3299, 3170, 2962, 2920, 2850, 1637, 1594, 1524, 1513, 1480, 1432, 1402, 1349, 1332, 1261, 1239, 1220, 1158, 1095 cm^{-1}.^{1}H NMR (600 MHz, $CDCl_3$, d): 8.20e8.19 (m, 2H, aromatic protons); 7.64e7.63 (m, 2H, aromatic protons); 7.18e7.15 (m, 2H, aromatic protons); 7.13e7.10 (m, 2H, aromatic protons); 4.70e4.62 (bs, 2H, NH_2: exchange with D_2O).^{13}C NMR (150 MHz, $CDCl_3$, d): 166.2, 162.2 (d, $^1J_{19F-13C}$ ¼ 248 Hz), 159.9, 148.4, 135.7, 131.1 (d, $^3J_{19F-13C}$ ¼ 8 Hz), 129.1, 123.8, 116.5 (d, $^2J_{19F-13C}$ ¼ 21 Hz), 100.0. GC-MS

(70 eV) m/z (rel. int.): 299 [M þ, 7], 150 (100), 123 (69), 104 (27), 103 (13), 86 (14), 85 (18), 77 (54), 76 (11), 63 (15), 51 (14). HRMS (ESI-TOF) m/z: [M þ Na]þ Calcd for $C_{15}H_{10}FN_3O_3Na$: 322.2664; Found 322.2666.

4-(4-Fluorophenyl)-3-[4-(methylsulfonyl)phenyl]isoxazol-5-amine (26). 31% yield. Mp 184e187 C (EtOAc/hexane). FT-IR (KBr): 3394, 3313, 3268, 3181, 2960, 2930, 2853, 1651, 1599, 1569, 1514, 1480, 1445, 1399, 1339, 1300, 1280, 1260, 1222, 1163, 1147, 1088, 1026, 959, 839, 787, 765, 748, 727, 606 cm^{1}.^{1}H NMR (600 MHz, $CDCl_3$, d): 7.92e7.91 (m, 2H, aromatic protons); 7.66e7.65 (m, 2H, aromatic protons); 7.18e7.15 (m, 2H, aromatic protons); 7.12e7.09 (m, 2H, aromatic protons); 4.70e4.65 (bs, NH_2: exchange with D_2O); 3.07 (s, 3H, CH_3).^{13}C NMR (150 MHz, $CDCl_3$, d): 166.1,162.1 (d, $^{1}J_{19F\text{-}13C}$ ¼ 248 Hz), 160.2, 141.2, 134.9, 131.1 (d, $^{3}J_{19F\text{-}13C}$ ¼ 8 Hz), 129.1, 127.6, 125.6 (d,$^{4}J_{19F\text{-}13C}$ ¼ 4 Hz), 116.5 (22 Hz), 93.4, 44.4.^{19}F NMR (470 MHz, $CDCl_3$, d): 115.4 (m). HRMS (ESI-TOF) m/z: [M þ Na]þ Calcd for $C_{16}H_{13}FN_2O_3SNa$: 355.3536; Found 355.3538.

Biology Materials. Cell culture reagents were purchased from EuroClone (Milan, Italy). RIPA buffer, protease inhibitor cocktail and CCK8, propidium iodide were obtained from Sigma- Aldrich (Milan, Italy). Anti-b-ACTIN, anti-COX-1 (COX-111), anti-COX-2 (COX-229), AnnexinV/Dead Cell Apoptosis kit were purchased from Thermo Fisher Scientific Italia (Monza, Italy). Anti-mouse secondary peroxidase antibody and all reagents for western blotting were purchased from Bio-Rad Laboratories Srl (Milan, Italy).

Cell Culture. The human NCI-H929 multiple myeloma (MM) cell line was purchased from The Leibniz Institute DSMZ (Germany). Human RPMI-8226 MM cell line was purchased from ATCC (Manassas, VA). NCI-H929 cells were grown in RPMI-1640 supplemented with 20% fetal bovine serum, 50 mM b-mercaptoethanol, 1 mM sodium pyruvate, 2 mM glutamine, 100 U/mL penicillin, 100 mg/mL streptomycin, in a humidified incubator at 37 C with a 5% CO_2 atmosphere. RPMI-8226 cells were grown in RPMI-1640 supplemented with 10% fetal bovine serum, 2 mM glutamine, 100 U/mL penicillin,100 mg/mL streptomycin, in a humidified incubator at 37 C with a 5% CO_2 atmosphere. HEK-293-derived cell lines stably and inducibly expressing hCOX-IRES-mPGES-1 were generated in tetracycline-inducible mammalian expression provided from W. L. Smith [41].

HEK-293 COX-1 and HEK-293 COX-2 were cultured in DMEM containing 10% no-deactivated fetal bovine serum, supplemented with 2 nM glutamine, hygromycin B (100 mg/mL), and blasticidin S (6.5 mg/mL) in a humidified incubator at 37 C with a 5% CO_2 atmosphere.

Cyclooxygenase activity inhibition determination. The final compounds were evaluated for their ability to inhibit ovine COX-1 or human COX-2 enzyme (percent inhibition at 50 mM). The inhibition of the enzyme was determined using a colorimetric COX inhibitor screening assay kit (Catalog No. 7601050, Cayman Chemicals, Ann Arbor, MI, USA) following the manufacturer's instructions. COX is a bifunctional enzyme exhibiting both cyclooxygenase and peroxidase activities. The cyclooxygenase component catalyzes the conversion of arachidonic acid into a hydroperoxide (PGG_2), and the peroxidase component catalyzes the reduction of endoperoxidase into the corresponding alcohol (PGH_2), the precursor of PGs, thromboxane and prostacyclin. The Colorimetric COX Inhibitor Screening Assay measures the peroxidase component of the cyclooxygenases. The peroxidase activity is colorimetrically assayed by monitoring the appearance of oxidized N,N,N^0,N^0 -tetramethyl-p-phenylenediamine (TMPD) at l ¼ 590 nm. Stock solutions of test compounds were dissolved in a minimum volume of DMSO.

Western Blotting. All cells were washed twice with 10 mL phosphate-buffered saline (PBS), scraped in 1 mL PBS and centrifuged for 10 min at 1500 rpm, 4 C. Proteins were extracted from cells by homogenization in cold RIPA buffer (Sigma-Aldrich) containing 1X protease inhibitor cocktail and centrifuged at 14,000 rpm for 10 min at 4 C. The supernatant was recovered, and the protein concentration was measured using DC Protein assay Reagent Kit (BIO-RAD). 30 mg of protein extract was separated on 10% polyacrylamide gel (BIO-RAD) and then transferred onto a polyvinylidene difluoride membrane (PVDF) by Trans-Blot Turbo Transfer System (BIO-RAD). Membrane was blocked for 1h at room temperature with blocking buffer (1% Blotting Grade Blocker, 0.1% Tween-20 in Tris-buffered saline, TBS). The membrane was then incubated with either anti- COX-1 (1:500 mouse monoclonal, overnight at 4 C), anti- COX-2 (1:500, mouse monoclonal, overnight at 4 C) or anti-b-actin (1:1000 mouse monoclonal, 1h at room temperature) antibodies, diluted in blocking buffer. After incubation time, membrane was washed with washing buffer (0.1% Tween-20 in Tris-buffered saline, TBS) for three times and incubated with a secondary peroxidase antibody (1:3000 anti-mouse) for 1h at room temperature. After washing, the membrane was treated with the enhanced chemiluminescence (ECL, BIO-RAD) according to the manufacturer's instructions and the blot was visualized by UVITEC Cambridge (Life Technologies). The expression level was evaluated by densitometric analysis using UVITEC Cambridge software (Life Technologies) and b-actin expression level was used as loading control to normalize the sample values.

Cell viability. Determination of cell growth was performed using the CCK8 assay at 48 h. On day 1, 50000 cells per well were seeded into 96-well plates in a volume of 50 mL. 7.9 nM for compound 1, 42 nM for compound 22 and 1.7 mM for aspirin (IC_{50} inhibitor activity). 2 nM in NCI-H929 and 3 nM in RPMI-8226 for bortezomib (EC_{50} cytotoxic activity). On day 2, 50 mL of the various drug concentrations were added. In all the experiments, the various drug-solvents (EtOH, DMSO) were added in each control to evaluate a possible solvent cytotoxicity. After 48 h incubation time with drugs, CCK8 (10 mL) was added to each well, and after 3e4 h incubation at 37 C, the absorbance values at l¼ 450 nm were determined on the microplate reader Victor 3 from PerkinElmer Life Sciences.

Cell cycle progression and apoptosis. MM cells in exponential growth were cultured in 6-wells plates of 10 cm^2 (1 10^6 cells/well) at 37 C in a 5% CO_2 atmosphere. After 24 h in complete medium, cells were exposed for 48 h to different concentrations of the tested isoxazoles depending on their IC_{50} or EC_{50} values. 7.9 nM for compound 1, 42 nM for compound 22 and 1.7 mM for aspirin (IC_{50} inhibitor activity). 2 nM in NCI-H929 and 3 nM in RPMI-8226 for bortezomib (EC_{50} cytotoxic activity). All controls were incubated with vehicle (DMSO). At the end of the treatment, cells were washed with PBS, centrifuged (2000 rpm, 10 min).

For cell cycle analysis, cells were fixed in 1 mL of ethanol at 70% ice. Samples containing 1 10^6 cells were centrifuged, rinsed in PBS, treated with 50 mg/mL RNase for 30 min at 37 C and then treated with 50 mg/mL Propidium iodide.

For apoptosis Dead Cell Apoptosis Kit with Annexin V Alexa Fluor™ 488 & Propidium Iodide (PI) (Catalog No: V13241, ThermoFisher) was used. Cells were suspended in 1X annexin-binding buffer to ~1 10^6 cells/mL 5 mL Alexa Fluor® 488 annexin V and 1 mL 100 mg/mL PI were added. Cells were incubated at room temperature for 15 min. After the incubation period, 400 mL 1X annexin-binding buffer were added. For both the experiments 50,000 cells were evaluated using a flow cytometer (Beckman coulter FC500).

Antiplatelet assays. Human platelet rich (PRP) and poor (PPP) plasma were prepared by differential centrifugation of fresh blood (n ¼ 3) (Ethics Committee e ID number: 2.364.834) and the platelet aggregation was monitored by turbidimetric method using Chronolog 560VS Aggregometer (Chrono-Log, Havertown, PA, USA). The

derivatives were pre-incubated in PRP for 2 min before addition of the arachidonic acid (AA - 500 mM) (Cayman Chemical Company, Ann Arbor, MI, USA). Different concentrations of the compounds were also tested to determine the concentration required to inhibit 50% of platelet aggregation (IC_{50}) induced by AA. The platelet aggregation tests were performed in triplicate and the positive controls was acetylsalicylic acid (ASA - 100 mM) (Sigma Aldrich, SP, Brazil) and the negative control was the vehicle 1% DMSO (Sigma Aldrich, SP, Brazil) [39,50].

Anticoagulant Assays. Human Platelet poor plasma (PPP) were prepared by differential centrifugation of fresh blood (n ¼ 3) (Ethics Committee e ID number: 2.364.834) and the assays were performed in coagulation analyzer CoagLab® IV (Beijing Shining Sun Technology Co. Ltd., China) as previously described by Sathler et al. [44]. In the APTT assay, plasma samples were first incubated with the compounds (100 mM) for 15 min at room temperature and them for 2 min at 37 C. Next, cephalin (100 mL) was added and incubated for 2 min. The reaction was triggered with 100 mL of 0.025 M $CaCl_2$ in a final volume of 300 mL. In the PT test, similarly, 97 mL of plasma were first incubated with the compounds for 15 min at room temperature and then 2 min at 37 C. Then 100 mL of PBS were added and incubated for 3 min. The reaction was triggered with 100 mL of calcium thromboplastin, in a final volume of 300 mL. The plasma clotting time was monitored in seconds at 37 C.

Hemolytic Activity. The hemolytic activity was investigated according to Parnham and Wetzig [51e53]. The citrated fresh blood (n ¼ 3) was centrifuged at 2500 rpm for 15 min and the erythrocyte pellet was washed 3 times with PBS (pH ¼ 7.4) and resuspended in same buffer (Ethics Committee e ID number: 2.364.834). Then the derivatives were incubated with the suspension of erythrocytes for 3h at 37 C in accord to ASTM F756-00 (Standard Practice for Assessment of Hemolytic Properties of Materials) [54]. The release of hemoglobin was measured after centrifugation of samples (2500 rpm for 15 min) and checked in a spectrophotometer at 540 nm. The complete hemolysis was obtained using 1% Triton X-100 as positive control. Less than 10% hemolysis was considered non-hemolytic [42].

Reverse Mutagenesis to Histidine Prototrophy (Ames Test). This assay was performed as described by Maron and Ames, using the histidine Salmonella typhimurium auxotroph mutant strains TA97, TA98, TA100 and the wild type strain TA102. Each assay was conducted in triplicate and the results obtained show a comparison between the molecules and the positive control 4-NQO. The negative results indicated that the molecules have no mutagenic properties. All compounds were tested at 500 mM [39].

SOS Chromotest-"Spot Test". The SOS chromotest (spot test) was performed according to Quillardet and Hofnung using Escherichia coli strains PQ35 and PQ37. One hundred microliters of an overnight culture of the E. coli strains are diluted in 5 mL of LB medium and the culture is incubated at 37 C in a gyratory incubator up to a concentration of 2 10^8 bacteria/mL. Fractions of 0.1 mL of the culture are then distributed into test tube with top agar, and the mixture is poured immediately on M63 medium plate. A sample of 10 mL of the molecules (500 mM) is spotted onto the center of the plate. After overnight incubation at 37 C, the presence of a blue ring around a zone of inhibition indicates genotoxic activity. Each assay was conducted in triplicate and the results obtained show a comparison between the molecules and the positive control 4-NQO.

Computational Methods. The computational tools employed are mainly part of FLAP package. The in silico procedure began with the design of the Mofezolac and 22 saved in minimized.mol2 format used in FLAP. Once the molecules were imported in FLAP, for each structure a maximum of 25 conformers were created, working at physiological pH conditions. FLAP was used in the structure-based mode and the template employed is the active site of the crystallographic structure: COX-1: mofezolac (PDB: 5WBE). The probes used in this analysis to generate the MIFs were the default probes DRY, O, N1 and H. It was then performed the "search for pockets" procedure, during which the system mimics the interactions between the default probes and the chemical environment of each amino acid present in the protein to recognize any active sites (protein pockets). The procedure was applied maintaining the default values (Number of additional trials ¼ 0, Sensitivity ¼ 6; Erosion ¼ 2) and without any constrains. FLAP compares the Molecular Interaction Fields (MIFs) of the cavity to those of the test compounds ranking the poses according to a similarity score.

5. Statistical analysis

Data were analyzed by applying the one-way repeated measures analysis of variants, and Bonferroni's multiple comparison test followed as a post hoc test. Results are reported as mean ± SD of three independent experiments, performed in triplicate. Statistical significance was accepted at $P < 0.05$.

Author contributions

The manuscript was written through contributions of all authors. All authors have given approval to the final version of the manuscript.

Acknowledgments

This work was supported by First Associazione Italiana per la Ricerca sul Cancro, Italia Grant-MFAG2015 (Project Id. 17566).

Appendix A. Supplementary data

Supplementary data to this article can be found online at https://doi.org/10.1016/j.ejmech.2018.12.029.

ABBREVIATIONS USED

AIBN	azobisisobutyronitrile
AA	arachidonic acid
BM	bone marrow
COX	cyclooxygenases
MM	multiple myeloma
NBS	N-bromosuccinimide
NSAIDs	Non-Steroidal Anti-inflammatory Drugs
PG	prostaglandin
SI	selectivity index
TBAF	tetrabutylammonium fluoride
TX	thromboxane

References

[1] M.G. Perrone, A. Scilimati, L. Simone, P. Vitale, Selective COX-1 inhibition: a therapeutic target to be reconsidered, Curr. Med. Chem. 17 (2010) 3769e3805.
[2] E. Ricciotti, G.A. FitzGerald, Prostaglandins and inflammation, Arterioscler. Thromb. Vasc. Biol. 31 (2011) 986e1000.
[3] M. Crescente, L. Menke, M.V. Chan, P.C. Armstrong, T.D. Warner, Eicosanoids in platelets and the effect of their modulation by aspirin in the cardiovascular system (and beyond), Br. J. Pharmacol. (2018).
[4] F. Finetti, R. Solito, L. Morbidelli, A. Giachetti, M. Ziche, S. Donnini, Prostaglandin E2 regulates angiogenesis via activation of fibroblast growth factor receptor-1, J. Biol. Chem. 283 (2008) 2139e2146.
[5] D. Wang, R.N. Dubois, Eicosanoids and cancer, Nat. Rev. Canc. 10 (2010) 181e193.
[6] N. Zidar, K. Odar, D. Glavac, M. Jerse, T. Zupanc, D. Stajer, Cyclooxygenase in normal human tissues e is COX-1 really a constitutive isoform, and COX-2 an

inducible isoform? J. Cell Mol. Med. 13 (2009) 3753e3763.
[7] M. Biava, Introduction to COX inhibitors, Future Med. Chem. 10 (2018) 1737e1740.
[8] M.G. Perrone, P. Vitale, S. Ferorelli, A. Boccarelli, M. Coluccia, A. Pannunzio, F. Campanella, G. Di Mauro, C. Bonaccorso, C.G. Fortuna, A. Scilimati, Effect of mofezolac-galactose distance in conjugates targeting cyclooxygenase (COX)-1 and CNS GLUT-1 Carrier, Eur. J. Med. Chem. 141 (2017) 404e416.
[9] R. Calvello, D.D. Lofrumento, M.G. Perrone, A. Cianciulli, R. Salvatore, P. Vitale, F. De Nuccio, L. Giannotti, G. Nicolardi, M.A. Panaro, A. Scilimati, Highly selective cyclooxygenase-1 inhibitors P6 and mofezolac counteract inflammatory state both in vitro and in vivo models of neuroinflammation, Front. Neurol. 8 (2017) 251e261.
[10] R. Calvello, M.A. Panaro, M.L. Carbone, A. Cianciulli, M.G. Perrone, P. Vitale, P. Malerba, A. Scilimati, Novel selective COX-1 inhibitors suppress neuroinflammatory mediators in LPS-stimulated N13 microglial cells, Pharmacol. Res. 65 (2012) 137e148.
[11] A.M. Rayar, N. Lagarde, C. Ferroud, J.F. Zagury, M. Montes, M. Sylla-Iyarreta Veitia, Update on COX-2 selective inhibitors: chemical classification, side effects and their use in cancers and neuronal diseases, Curr. Top. Med. Chem. 17 (2017) 2935e2956.
[12] G. Carullo, F. Galligano, F. Aiello, Structureeactivity relationships for the synthesis of selective cyclooxygenase 2 inhibitors: an overview (2009e2016), MedChemComm 8 (2017) 492e500.
[13] M. Fahlen, H. Zhang, L. Lofgren, B. Masironi, E. von Schoultz, B. von Schoultz, L. Sahlin, Expression of cyclooxygenase-1 and cyclooxygenase-2, syndecan-1 and connective tissue growth factor in benign and malignant breast tissue from premenopausal women, Gynecol. Endocrinol. 33 (2017) 353e358.
[14] M.G. Perrone, P. Malerba, J. Uddin, P. Vitale, A. Panella, B.C. Crews, C.K. Daniel, K. Ghebreselasie, M. Nickels, M.N. Tantawy, H.C. Manning, L.J. Marnett, A. Scilimati, PET radiotracer [^{18}F]-P6 selectively targeting COX-1 as a novel biomarker in ovarian cancer: preliminary investigation, Eur. J. Med. Chem. 80 (2014) 562e568.
[15] B.M. Erovic, M. Woegerbauer, J. Pammer, E. Selzer, M.Ch Grasl, D. Thurnher, Strong evidence for up-regulation of cyclooxygenase-1 in head and neck cancer, Eur. J. Clin. Investig. 38 (2008) 61e66.
[16] W.M. Osman, N.S. Youssef, Combined use of COX-1 and VEGF immunohistochemistry refines the histopathologic prognosis of renal cell carcinoma, Int. J. Clin. Exp. Pathol. 8 (2015) 8165e8177.
[17] J. Ding, K. Tsuboi, H. Hoshikawa, R. Goto, N. Mori, M. Katsukawa, E. Hiraki, S. Yamamoto, M. Abe, N. Ueda, Cyclooxygenase isozymes are expressed in human myeloma cells but not involved in anti-proliferative effect of cyclooxygenase inhibitors, Mol. Carcinog. 45 (2006) 250e259.
[18] R.L. Siegel, K.D. Miller, A. Jemal, Cancer statistics, 2018. CA, Cancer J. Clin. 68 (2018) 7e30.
[19] D. Chauhan, Z. Tian, B. Nicholson, K.G. Kumar, B. Zhou, R. Carrasco, J.L. McDermott, C.A. Leach, M. Fulcinniti, M.P. Kodrasov, J. Weinstock, W.D. Kingsbury, T. Hideshima, P.K. Shah, S. Minvielle, M. Altun, B.M. Kessler, R. Orlowski, P. Richardson, N. Munshi, K.C. Anderson, A small molecule inhibitor of ubiquitin-specific protease-7 induces apoptosis in multiple myeloma cells and overcomes bortezomib resistance, Cancer Cell 22 (2012) 345e358.
[20] G.J. Morgan, F.E. Davies, Role of thalidomide in the treatment of patients with multiple myeloma, Crit. Rev. Oncol. Hematol. 1 (2013) S14eS22.
[21] T. Bagratuni, E. Kastritis, M. Politou, M. Roussou, E. Kostouros, M. Gavriatopoulou, E. Eleutherakis-Papaiakovou, N. Kanelias, E. Terpos, M.A. Dimopoulos, Clinical and genetic factors associated with venous thromboembolism in myeloma patients treated with lenalidomide-based regimens, Am. J. Hematol. 88 (2013) 765e770.
[22] G.H. Lyman, K. Bohlke, A. Falanga, Venous thromboembolism prophylaxis and treatment in patients with cancer: American Society of Clinical Oncology clinical practice guideline update, J. Oncol. Pract. Am. Soc. Clin. Oncol. 11 (2015) 442e444.
[23] P. Sonneveld, A. Broijl, Treatment of relapsed and refractory multiple myeloma, Haematologica 101 (2016) 995.
[24] J. Ding, L. Yuan, G. Chen, Aspirin enhances the cytotoxic activity of bortezomib against myeloma cells via suppression of Bcl-2, survivin and phosphorylation of AKT, Oncology Letters 13 (2017) 647e654.
[25] V. Evangelista, S. Manarini, A. Di Santo, M.L. Capone, E. Ricciotti, L. Di Francesco, S. Tacconelli, A. Sacchetti, S. D'Angelo, A. Scilimati, M.G. Sciulli, P. Patrignani, De novo synthesis of Cyclooxygenase-1 counteracts the suppression of platelet thromboxane biosynthesis by aspirin, Circ. Res. 98 (2006) 593e595.
[26] P. Lambrakis, G.F. Rushworth, J. Adamson, S.J. Leslie, Aspirin hypersensitivity and desensitizaion protocols: implications for cardiac patients, Ther. Adv. Drug Saf. 2 (2011) 263e270.
[27] L. Di Nunno, P. Vitale, A. Scilimati, S. Tacconelli, P. Patrignani, Novel synthesis of 3,4-diarylisoxazole analogues of valdecoxib: reversal cyclooxygenase-2 selectivity by sulfonamide group removal, J. Med. Chem. 47 (2004) 4881e4890.
[28] G. Cingolani, A. Panella, M.G. Perrone, P. Vitale, G. Di Mauro, C.G. Fortuna, R.S. Armen, S. Ferorelli, W.L. Smith, A. Scilimati, Structural basis for selective inhibition of Cyclooxygenase-1 (COX-1) by diarylisoxazoles mofezolac and 3-(5-chlorofuran-2-yl)-5-methyl-4-phenylisoxazole (P6), Eur. J. Med. Chem. 138 (2017) 661e668.
[29] M.G. Perrone, P. Vitale, P. Malerba, A. Altomare, R. Rizzi, A. Lavecchia, C. Di Giovanni, E. Novellino, A. Scilimati, Diarylheterocycle core ring features effect in selective COX-1 inhibition, ChemMedChem 7 (2012) 629e641.
[30] M.G. Perrone, P. Vitale, A. Panella, S. Ferorelli, M. Contino, A. Lavecchia, A. Scilimati, Isoxazole-based-scaffold inhibitors targeting cyclooxygenases (COXs), ChemMedChem 11 (2016) 1172e1187.
[31] M.G. Perrone, P. Vitale, A. Panella, C.G. Fortuna, A. Scilimati, General role of the amino and methylsulfamoyl groups in selective cyclooxygenase(COX)-1 inhibition by 1,4-diaryl-1,2,3-triazoles and validation of a predictive pharmacometric PLS model, Eur. J. Med. Chem. 13 (94) (2015) 252e264.
[32] P. Vitale, S. Tacconelli, M.G. Perrone, P. Malerba, L. Simone, A. Scilimati, A. Lavecchia, M. Dovizio, E. Marcantoni, A. Bruno, P. Patrignani, Synthesis, pharmacological characterization, and docking analysis of a novel family of diarylisoxazoles as highly selective cyclooxygenase-1 (COX-1) inhibitors, J. Med. Chem. 56 (2013) 4277e4299.
[33] G. Casalino, M. Coluccia, M.L. Pati, A. Pannunzio, A. Scilimati, M.G. Perrone, Intelligent microarray data analysis through Non-negative Matrix Factorization to study Human Multiple Myeloma cell lines, BMC Bionformatics (2019) (submitted for pubblication).
[34] P.C. Armstrong, N.S. Kirkby, Z.N. Zain, M. Emerson, J.A. Mitchell, T.D. Warner, Thrombosis is reduced by inhibition of COX-1, but unaffected by inhibition of COX-2, in an acute model of platelet activation in the mouse, PLoS One 6 (2011), e20062.
[35] P. Vitale, M.G. Perrone, P. Malerba, A. Lavecchia, A. Scilimati, Selective COX-1 inhibition as a target of theranostic novel diarylisoxazoles, Eur. J. Med. Chem. 74 (2014) 606e618.
[36] P. Vitale, A. Scilimati, Functional 3-arylisoxazoles and 3-aryl-2-isoxazolines from reaction of aryl nitrile oxides and enolates: synthesis and reactivity, Synthesis 45 (2013) 2940e2948.
[37] P. Vitale, A. Scilimati, Recent developments in the chemistry of 3-arylisoxazoles and 3-Aryl-2-isoxazolines, in: Eric F.V. Scriven, Christopher A. Ramsden (Eds.), Advances in Heterocyclic Chemistry, 122, 2017, pp. 1e41.
[38] M. Baroni, G. Cruciani, S. Sciabola, F. Perruccio, J.S. Mason, A common reference framework for analyzing/comparing proteins and ligands. Fingerprints for ligands and proteins (FLAP): theory and application, J. Chem. Inf. Model. 47 (2007) 279e294.
[39] A.L. Lourenço, R.R.S. Salvador, L.A. Silva, M.S. Saito, J.F.R. Mello, L.M. Cabral, C.R. Rodrigues, M.A.F. Vera, E.M.F. Muri, A.M.T. de Souza, C.S. Craik, L.R.S. Dias, H.C. Castro, P.C. Sathler, Synthesis and mechanistic evaluation of novel N'-benzylidene-carbohydrazide-1H-pyrazolo[3,4-b]pyridine derivatives as non-anionic antiplatelet agents, Eur. J. Med. Chem. 135 (2017) 213e229.
[40] K.V. Sashidhara, G.R. Palnati, S.R. Avula, S. Singh, M. Jain, M. Dikshit, Synthesis and evaluation of anti-thrombotic activity of benzocoumarin amide derivatives, Bioorg. Med. Chem. Lett 22 (2012) 3115e3121.
[41] A.L. Lourenço, M.S. Saito, L.E. Dorneles, G.M. Viana, P.C. Sathler, L.C. Aguiar, M. de Padula, T.F. Domingos, A.G. Fraga, C.R. Rodrigues, V.P. de Sousa, H.C. Castro, L.M. Cabral, Synthesis and antiplatelet activity of antithrombotic thiourea compounds: biological and structure-activity relationship studies, Molecules 20 (2015) 7174e7200.
[42] D. Fischer, Y. Li, B. Ahlemeyer, J. Krieglstein, T. Kissel, In vitro cytotoxicity testing of polycations: influence of polymer structure on cell viability and hemolysis, Biomaterials 24 (2003) 1121e1131.
[43] C. Yuan, W.L. Smith, A cyclooxygenase-2-dependent prostaglandin E2 biosynthetic system in the golgi apparatus, J. Biol. Chem. 290 (2015) 5606e5620.
[44] P. Vitale, L. Di Nunno, A. Scilimati, A novel synthesis of N-unsubstituted ß-enamino thioesters from 3-arylisoxazoles and 3-aryl-5-phenylthio-2-isoxazolines, Synthesis 18 (2010) 3195e3203.
[45] A. Salomone, A. Scilimati, P. Vitale, 3-Aryl-5-vinyl-2-isoxazolines and 3-aryl-5-vinylisoxazoles from aryl nitrile oxides and methyl vinyl ketone lithium enolate: reaction limits and synthetic utility exploitation, Synthesis 47 (2015) 807e816.
[46] L. Di Nunno, P. Vitale, A. Scilimati, L. Simone, F. Capitelli, Stereoselective dimerization of 3-arylisoxazoles to cage-shaped bis-beta-lactams syn 2,6-diaryl-3,7-diazatricyclo[4.2.0.02,5]-octan-4,8-diones induced by hindered lithium amides, Tetrahedron 63 (2007) 12388e12395.
[47] L. Di Nunno, A. Scilimati, P. Vitale, Regioselective synthesis and side-chain metalation and elaboration of 3-aryl-5-alkylisoxazoles, Tetrahedron 58 (2002) 2659e2665.
[48] L. Di Nunno, P. Vitale, A. Scilimati, Effect of the aryl group substituent in the dimerization of 3-arylisoxazoles to syn 2,6-diaryl-3,7-diazatricyclo[4.2.0.02,5]octan-4,8-diones induced by LDA, Tetrahedron 64 (2008) 11198e11204.
[49] P. Vitale, A. Scilimati, Five-membered ring heterocycles by reacting enolates with dipoles, Curr. Org. Chem. 17 (18) (2013) 1986e2000.
[50] P.C. Sathler, A.L. Lourenço, C.R. Rodrigues, L.C.R.P. da Silva, L.M. Cabral, A.K. Jordao, et al., In vitro and in vivo analysis of the antithrombotic and toxicological profile of new antiplatelets N-acylhydrazone derivatives and development of nanosystems: determination of novel NAH derivatives antiplatelet and nanotechnological approach, Thromb. Res. 134 (2014) 376e383.
[51] M. Bauer, C. Lautenschlaeger, K. Kempe, L. Tauhardt, U.S. Schubert, D. Fischer, Poly(2-ethyl-2-oxazoline) as alternative for the stealth polymer poly(ethylene glycol): comparison of in vitro cytotoxicity and hemocompatibility,

Macromol. Biosci. 12 (2012) 986e998.
[52] A. Catalano, A. Carocci, F. Corbo, C. Franchini, M. Muraglia, et al., Constrained analogues of tocainide as potent skeletal muscle sodium channel blockers towards the development of antimyotonic agents, Eur. J. Med. Chem. 43 (2008) 2535e2540.
[53] P. Vitale, F.M. Perna, M.G. Perrone, A. Scilimati, Screening on the use of Kluyveromyces marxianus CBS 6556 growing cells as enantioselective bio-catalysts for ketone reductions, Tetrahedron Asymmetry 22 (2011) 1985e1993.
[54] F04 Committee, Practice for Assessment of Hemolytic Properties of Materials, ASTM International, 2013.